Different complex regulatory phenotypes underlie hybrid male sterility in divergent rodent crosses

Kelsie E. Hunnicutt[*,1], Colin Callahan[2], Sara Keeble[2], Emily C. Moore[1,2], Jeffrey M. Good[2], and Erica L. Larson[*,1]

[1] University of Denver, Department of Biological Sciences, Denver, CO, 80208
[2] Division of Biological Sciences, University of Montana, Missoula, MT, 59812
*Corresponding authors

ORCID: 0000-0002-9674-0630 (KEH)
ORCID: 0000-0002-0385-1121 (CC)
ORCID: 0000-0002-7318-3122 (SK)
ORCID: 0000-0001-6166-3367 (ECM)
ORCID: 0000-0003-0707-5374 (JMG)
ORCID: 0000-0003-3006-645X (ELL)

Corresponding Authors:
Kelsie Hunnicutt
Department of Biological Sciences
University of Denver
Denver, CO 80208
Email: Kelsie.Hunnicutt@du.edu

Erica Larson
Department of Biological Sciences
University of Denver
Denver, CO 80208
Email: Erica.Larson@du.edu

Running title: Rodent hybrid male sterility

Key words: speciation, hybrid male sterility, gene expression, fluorescence activated cell sorting, meiotic sex chromosome inactivation, *Phodopus*

ABSTRACT

Hybrid incompatibilities are a critical component of species barriers and may arise due to negative interactions between divergent regulatory elements in parental species. We used a comparative approach to identify common themes in the regulatory phenotypes associated with hybrid male sterility in two divergent rodent crosses, dwarf hamsters and house mice. We investigated three potential characteristic gene expression phenotypes in hybrids including the propensity of transgressive differentially expressed genes towards over or underexpression, the influence of developmental stage on patterns of misexpression, and the role of the sex chromosomes on misexpression phenotypes. In contrast to near pervasive overexpression in hybrid house mice, we found that misexpression in hybrid dwarf hamsters was dependent on developmental stage. In both house mouse and dwarf hamster hybrids, however, misexpression increased with the progression of spermatogenesis, although to varying extents and with potentially different consequences. In both systems, we detected sex-chromosome specific overexpression in stages of spermatogenesis where inactivated X chromosome expression was expected, but the hybrid overexpression phenotypes were fundamentally different. Importantly, misexpression phenotypes support the presence of multiple developmental blocks to spermatogenesis in dwarf hamster hybrids, including a potential role of meiotic stalling or breakdown early in spermatogenesis. Collectively, we demonstrate that while there are some similarities in hybrid expression phenotypes of house mice and dwarf hamsters, there are also clear differences that point towards unique mechanisms underlying hybrid male sterility. Our results highlight the potential of comparative approaches in helping to understand the causes and consequences of disrupted gene expression in speciation.

INTRODUCTION

The evolution of postzygotic reproductive barriers, such as hybrid inviability and sterility, is an important part of the speciation process, and identifying the genetic architecture of hybrid incompatibilities has been a common goal uniting speciation research (Coughlan and Matute 2020). While identifying the genetic basis of hybrid dysfunction remains difficult in many systems, downstream regulatory phenotypes can provide insight into the underlying mechanisms of speciation (Mack and Nachman 2017). An outstanding question surrounding the role of disrupted gene regulation and speciation is whether the combination of two divergent genomes in hybrids results in gene expression perturbations that are consistent or repeatable across species. At the broadest level, it is unclear whether gene expression in hybrids tends to be intermediate or transgressive (outside the range of parental gene expression), whether transgressive gene expression is biased towards over or underexpression (Ortíz-Barrientos *et al.* 2007), and whether transgressive misexpression tends to be modulated by *cis* or *trans* regulatory elements (Wittkopp *et al.* 2004; McManus *et al.* 2010; Oka *et al.* 2014; Mack *et al.* 2016; Mugal *et al.* 2020; Kopania *et al.* 2022a). By investigating trends in the magnitude and direction of transgressive expression across different hybrid systems, we can begin to understand the evolutionary forces shaping regulatory-based hybrid incompatibilities. For example, if transgressive misexpression in hybrids tends towards overexpression, this may mean that genes with disrupted regulation in hybrids tend to be genes that are normally repressed in parental lineages (Meiklejohn *et al.* 2014; Barreto *et al.* 2015; Larson *et al.* 2017). Alternatively, transgressive misexpression in hybrids may tend towards underexpression if regulatory divergence between parental lineages results in impaired transcription factor binding with promoter or enhancer elements (Oka *et al.* 2014; Guerrero *et al.* 2016) or if divergence stimulates epigenetic silencing (Paun *et al.* 2007; Shivaprasad *et al.* 2012; Lafon-Placette and

Köhler 2015; Brekke *et al.* 2016; Zhu *et al.* 2017). At a finer scale, transgressive misexpression patterns may depend on developmental stage: for example, if there is greater pleiotropy earlier in development (Ortíz-Barrientos *et al.* 2007; Cutter and Bundus 2020). In particular, we might expect sterile hybrids to have more transgressive misexpression during later stages of gametogenesis when genes are evolving rapidly and are potentially under less regulatory constraint (Kopania *et al.* 2022a; Murat *et al.* 2023). Finally, the role of sex chromosome regulation in inviable or sterile hybrids encompasses both larger questions. Sex chromosomes may be prone to asymmetry in their expression divergence (Oka and Shiroishi 2014; Civetta 2016) and be regulated differently across stages of development (Presgraves 2008; Larson *et al.* 2018), particularly in reproductive tissues, and thus may play a central role in hybrid dysregulation relative to autosomes.

Disruption of sex chromosome regulation is thought to be a potentially widespread regulatory phenotype in sterile hybrids (Lifschytz and Lindsley 1972; Larson *et al.* 2018), in part because X chromosome repression may be crucial to normal spermatogenesis in diverse taxa (McKee and Handel 1993; Landeen *et al.* 2016; Taxiarchi *et al.* 2019; Rappaport *et al.* 2021; Viera *et al.* 2021; Murat *et al.* 2023). Furthermore, misregulation of the X chromosome is associated with hybrid sterility in several species pairs (Davis *et al.* 2015; Sánchez-Ramírez *et al.* 2021; Bredemeyer *et al.* 2021), although it has been best studied in house mice. In fertile male mice, the X chromosome is silenced just prior to the Diplotene stage of meiosis through meiotic sex chromosome inactivation (MSCI; McKee and Handel 1993; Handel 2004) and is again repressed in postmeiotic sperm development (*i.e.,* postmeiotic sex chromosome repression or PSCR; Namekawa *et al.* 2006). In contrast, the X chromosome is not properly inactivated and is overexpressed in sterile hybrid mice (Good *et al.* 2010; Bhattacharyya *et al.* 2013; Campbell *et al.* 2013; Turner *et al.* 2014; Larson *et al.* 2017, 2022). Disrupted MSCI in house mice is associated with divergence at *Prdm9*, a gene that is a major contributor to

74 hybrid male sterility (Mihola *et al.* 2009; Davies *et al.* 2016). However, misexpression of the X
75 chromosome in sterile hybrids could result from mechanisms other than *Prdm9*-associated
76 disrupted MSCI, such as mispairing of the sex chromosomes due to divergence in their region
77 of homology known as the pseudoautosomal region (PAR; Burgoyne 1982; Ellis and
78 Goodfellow 1989; Raudsepp and Chowdhary 2015). In sum, the ubiquity of X chromosome
79 repression and the growing body of evidence linking disrupted MSCI to hybrid sterility in
80 mammals suggest that disrupted sex chromosome regulation may be a common regulatory
81 phenotype in sterile hybrid males.

82 Here, we characterized disruption of gene expression associated with hybrid male
83 sterility in two rodent crosses, dwarf hamsters and house mice, which span ~35 million years
84 of divergence (Swanson *et al.* 2019). The regulatory phenotypes of hybrid male sterility have
85 been thoroughly studied in house mice (Good *et al.* 2010; Bhattacharyya *et al.* 2013; Campbell
86 *et al.* 2013; Turner *et al.* 2014; Larson *et al.* 2017, 2022; Hunnicutt *et al.* 2022). We contrast
87 these with an analogous cross between two sister species of dwarf hamster, Campbell's dwarf
88 hamster (*Phodopus campbelli*) and the Siberian dwarf hamster (*P. sungorus*), and their sterile
89 F1 hybrid male offspring. These species diverged only ~0.8-1.0 million years ago (Neumann *et*
90 *al.* 2006), and they are not thought to interbreed in the wild due to geographic separation
91 (Ishishita *et al.* 2015). Crosses between female *P. sungorus* and male *P. campbelli* produce
92 sterile hybrid males that, similar to mice, have a range of sterility phenotypes, suggesting
93 multiple developmental blocks to spermatogenesis (Ishishita *et al.* 2015; Bikchurina *et al.*
94 2018). Hybrids from the reciprocal cross are usually inviable due to abnormal growth *in utero*
95 (Brekke and Good 2014), and the species origin of the X chromosome is the primary genetic
96 factor controlling hybrid inviability (Brekke *et al.* 2021). Additionally, sex chromosome
97 asynapsis during spermatogenesis is common in hybrid dwarf hamsters, providing further
98 reason to think that X chromosome-specific misregulation may be observed in sterile hybrid

99 dwarf hamsters (Ishishita *et al.* 2015; Bikchurina *et al.* 2018). Both the abnormal spermatogenic
100 phenotypes observed in dwarf hamster hybrids and the potential regulatory interactions that
101 may result from the involvement of the X chromosome in multiple reproductive barriers make
102 dwarf hamsters an important comparison to mice for investigating what regulatory phenotypes
103 may be repeatedly associated with the evolution of postzygotic reproductive isolation.

104 Expression phenotypes associated with hybrid sterility have historically been difficult to
105 assess because of the cellular diversity of reproductive tissues (*e.g.,* testes; Ramm and
106 Schärer 2014) and because hybrids may differ from parents in both tissue composition and
107 developmental timing (reviewed in Montgomery and Mank 2016; Hunnicutt *et al.* 2022). To
108 overcome these difficulties, we used Fluorescence Activated Cell Sorting (FACS) to isolate and
109 sequence cell populations across the developmental timeline of spermatogenesis for each
110 species pair and their F1 hybrids, including stages that span the different sex chromosome
111 regulatory states. Our developmental timeline spans stages where we expect fertile parents to
112 have a transcriptionally active X chromosome (spermatogonia and leptotene/zygotene
113 spermatocytes) and an inactive X chromosome (diplotene spermatocytes and round
114 spermatids). We used both datasets to address three main questions about the transgressive
115 gene expression phenotypes observed in sterile hybrids: (1) within transgressive differentially
116 expressed genes, does misexpression tend towards up- or downregulation in hybrids
117 compared to parents? (2) are there similar patterns of disrupted transgressive expression
118 across stages of development? and (3) are there clear differences between autosomes and sex
119 chromosomes in expression phenotypes? And if so, is sex chromosome-specific transgressive
120 misexpression consistent with either disrupted MSCI and/or disrupted PAR regulation?
121 Collectively, we demonstrate the power of cell type-specific approaches for untangling the
122 expression phenotypes associated with the evolution of hybrid male sterility and for identifying
123 common themes in the mechanistic basis of hybrid incompatibilities across divergent taxa.

124 **MATERIALS AND METHODS**

125 **Hamster crosses and male reproductive phenotypes**

126 We used wild-derived colonies of two sister species of dwarf hamster, *P. sungorus* and
127 *P. campbelli*, established by Kathy Wynne-Edwards (Scribner and Wynne-Edwards 1994) and
128 housed at the University of Montana. Both species were maintained as closed colonies with a
129 breeding scheme to minimize inbreeding. Nonetheless, inbreeding levels of these closed
130 colonies are still high as indicated by very low nucleotide diversity (Brekke *et al.* 2018). We
131 used males from both parent species and male F1 hybrid offspring from crosses of female *P.*
132 *campbelli* with male *P. sungorus*. We weaned males in same-sex sibling groups between 17 -
133 21 dpp and housed them individually at 45 dpp. We euthanized reproductively mature males
134 using carbon dioxide followed by cervical dislocation between 59 - 200 dpp (Table S1 in File
135 S1). All animal use was approved by the University of Montana (IACUC protocols 050-
136 16JGDBS & 035-19JGDBS).

137 We measured several fertility metrics for parent species and hybrid males including
138 paired testes weight, paired seminal vesicle weight, normalized sperm counts, and sperm
139 motility (Good *et al.* 2008). Paired testes weight and paired seminal vesicle weight were
140 correlated with body weight (paired testes weight Pearson's $r(29) = 0.47$, $p = 0.007$; paired
141 seminal vesicle weight Pearson's $r(23) = 0.56$, $p = 0.003$), so we standardized both metrics
142 relative to body weight. We calculated sperm count by isolating sperm from caudal
143 epididymides diced in 1 ml of Dulbecco's PBS (Sigma) and incubated at 37°C for 10 minutes.
144 We quantified sperm motility (proportion of motile sperm in a 5 µl suspension) and sperm count
145 (number of sperm with head and tail in a heat shocked 5 µl suspension) across a fixed area on
146 a Makler counting chamber. We performed statistical comparisons of fertility phenotypes in R

147 v.4.3.1, and we used the FSA package v.0.9.4 for the Kruskal-Wallis and Dunn's tests (Ogle
148 and Ogle 2017).
149
150 **Isolation of enriched cell populations from hamster testes**
151 To investigate the regulatory dynamics of the sex chromosomes during
152 spermatogenesis, we isolated four spermatogenic cell populations from whole testes using
153 FACS. These cell populations span a developmental timeline of spermatogenesis from mitosis
154 (spermatogonia), meiosis prior to X inactivation (leptotene/zygotene spermatocytes), meiosis,
155 after X inactivation (diplotene spermatocytes), and post-meiosis (round spermatids). Briefly, we
156 disassociated a single testis per male following a published protocol originally developed for
157 house mice (Getun *et al.* 2011) with modifications (github.com/goodest-goodlab/good-
158 protocols/tree/main/protocols/FACS, last accessed June 16, 2021). We doubled the volumes
159 of all reagents to account for the increased mass of testes in dwarf hamsters relative to house
160 mice. We isolated cell populations based on size, granularity, and fluorescence on a FACSAria
161 IIu cell sorter (BD Biosciences) at the University of Montana Center for Environmental Health
162 Sciences Fluorescence Cytometry Core. For each sorted cell population, we extracted RNA
163 using RNeasy kits (Qiagen) following protocols for Purification of Total RNA from Animal Cells.
164 We quantified sample RNA quantity and quality (requiring an RNA integrity number > 7) on a
165 Tapestation 2200 (Agilent) at the University of Montana genomics core. RNA libraries were
166 prepared by Novogene and sequenced on Illumina NovaSeq 6000s (paired end, 150 bp). Six
167 samples (distributed across different species and cell types) had low RNA concentrations, and
168 for these samples we used Novogene's low input RNA library preparation (Table S2 in File S1).
169 MDS plots indicated no severe library batch effects between samples from different library
170 preparations (Figure S1 in File S1), so we included all samples from both libraries in
171 subsequent analyses.

Read processing and mapping

We sequenced RNA from each cell population for three to five individuals of each parent species and F1 hybrids generating an average of ~27.5 million read pairs per individual (Table S2 in File S1). We trimmed reads using Trimmomatic v.0.39 (Bolger *et al.* 2014) to remove low quality bases from the first and last 5 bp of each read and bases with an average Phred score of less than 15 across a 4 bp sliding window and only retained reads of at least 36 bp. We next used an approach (based on the modtools pipeline) which maps reads from each sample to pseudogenomes for both parent species (described below) to obtain a merged output alignment file in order to alleviate reference bias associated with mapping hybrids to only a single reference genome (Holt *et al.* 2013; Huang *et al.* 2014). For this approach, we mapped reads for each individual to both a *P. sungorus* pseudogenome and a *P. campbelli* pseudogenome with Hisat v.2.2.0 (Kim *et al.* 2019) with default settings and retaining at most 100 distinct, primary alignments, although multi-mapped reads were removed downstream (described below). We generated the *P. sungorus* pseudogenome by mapping RNASeq reads from a male *P. sungorus* individual (30.6 million total read pairs; NCBI SRA: SRR17223284; Moore *et al.* 2022) to the *P. sungorus* reference genome (GCA_023856395.1) with bwa-mem v.2.2.1 (Vasimuddin *et al.* 2019), and the *P. campbelli* pseudogenome by mapping female *P. campbelli* whole genome sequencing reads (average coverage: 33x; NCBI SRA: SRR17223279; Moore *et al.* 2022) to the *P. sungorus* reference genome. Because our *P. sungorus* pseudogenome was based on a male hamster and the reference genome on a female hamster, we excluded reads mapping to the PAR because sequences mapping to this region could have originated from either the X or Y chromosomes and interfered with subsequent variant calling. Following mapping, we used GATK v.4.2.5.0 HaplotypeCaller (-ERC GVCF) to call SNPs then performed genotyping with genotypeGVCFs. We hard-filtered our SNPs (--mask-extension 5 "QD < 2.0" "FS > 60.0" "MQ < 40.0" "QUAL < 30.0" "DP < 10" "DP > 150") and restricted

197 SNPs to biallelic loci. Finally, we incorporated filtered SNPs back into the *P. sungorus*
198 reference genome with FastaAlternateReferenceMaker to create the *P. sungorus* and *P.*
199 *campbelli* pseudoreferences. For our RNASeq data, we appended query hit indexes to
200 resulting alignment files using hisat2Tophat.py (https://github.com/goodest-goodlab/pseudo-
201 it/tree/master/helper-scripts/hisat2Tophat.py, last accessed March 8th, 2022) to maintain
202 compatibility with the modtools pipeline. We used our VCFs (above) to generate a mod-file for
203 both species with vcf2mod from Lapels v.1.1.1 to convert alignments to the *P. sungorus*
204 reference genome, and Suspenders v.0.2.6 to merge alignments while retaining the highest
205 quality alignment per read (Holt *et al.* 2013; Huang *et al.* 2014). We used featureCounts v.2.0.1
206 (Liao *et al.* 2014) to estimate counts of read pairs that aligned to the same chromosome (-B
207 and -C) and retained only singly-mapped reads. Summaries of properly mapped reads for each
208 sample can be found in Table S2 in File S1.

209 We sought to compare the gene expression phenotypes observed in dwarf hamsters to
210 those previously documented in house mice using published RNASeq data for the same four
211 spermatogenic cell types of two subspecies of house mouse and their sterile F1 hybrids
212 (Larson *et al.* 2017; Hunnicutt *et al.* 2022). These studies examined two subspecies of house
213 mice, *Mus musculus musculus* (intra-subspecific F1 males between wild-derived inbred strains
214 PWK/PhJ♀ and CZECHII/EiJ♂) and *M. m. domesticus* (intra-subspecific F1 males between
215 wild-derived inbred strains WSB/EiJ♀ and LEWES/EiJ♂) and their sterile (PWK♀ x LEWES♂)
216 F1 hybrids for disrupted gene expression across spermatogenesis following the same FACS
217 protocols implemented in this study. For all comparisons between house mice and dwarf
218 hamsters, we used read count files generated previously for house mice (Hunnicutt *et al.* 2022)
219 and performed all subsequent analyses in parallel for both systems.
220

221 **Estimating nucleotide diversity and divergence within and between crosses and strains**
222
223 We next estimated nucleotide diversity within and divergence between each strain or
224 cross for parent species and hybrids (π and d_{XY}). We used the bam files generated above from
225 mapping each strain or cross to its respective reference genome (either GCA_023856395.1 for
226 dwarf hamsters or GRCm38.p6 for house mice) to call SNPs as described above but with the
227 addition of a step to split reads at intronic regions using the GATK function SplitNCigarReads.
228 We generated two VCFs, one for dwarf hamster crosses and the other for house mouse
229 crosses, which we processed and filtered separately. If an individual mouse or hamster was
230 sequenced for more than one cell type, we randomly chose one of the represented cell types
231 to be included in the analysis. We hard-filtered our SNPs as above and restricted SNPs to
232 biallelic loci. Because our SNPs were called from RNASeq data and thus may be susceptible to
233 allelic imbalances or coverage differences between samples, we next investigated how the
234 inclusion of SNPs with different levels of missing data impacted estimation of π and d_{XY}. We
235 used vcftools v.0.1.17 (Danecek *et al.* 2011) to filter SNPs allowing between 0% and 90%
236 missing data (--max_missing; Figure S3 in File S1), and filtered SNPs with a depth lower than 5
237 and higher than 60 (~2-3 higher than average coverage) to eliminate multi-mapped reads.
238 Finally, we used pixy v.1.2.10.beta2 (Korunes and Samuk 2021) on our filtered VCFs to
239 estimate π and d_{XY}. Patterns of nucleotide diversity across strains and crosses were
240 qualitatively similar across missing data thresholds, so we present results corresponding to
241 10% missing data in the main text. However, we note that for all comparisons, estimates of π
242 and d_{XY} decreased with more stringent missing data thresholds regardless of strain or cross
243 (Figure S3 in File S1).
244

245 **Gene expression pre-processing**

246 Following read processing and mapping, we conducted all analyses in R v.4.3.1. We
247 classified genes as “expressed” if genes had a minimum of one Fragment Per Kilobase of exon
248 per Million mapped reads (FPKM) in at least three samples, resulting in 21,077 expressed
249 genes across the dwarf hamster dataset and 21,212 expressed genes across the house mouse
250 dataset. We also identified sets of genes “induced” in a given cell type defined as genes with a
251 median expression in a given cell population (normalized FPKM) greater than two times its
252 median expression across all other sorted cell populations (following Kousathanas *et al.* 2014).
253 We calculated normalized FPKM values by adjusting the sum of squares to equal one using the
254 R package vegan v.2.6-4 (Oksanen *et al.* 2013). We conducted expression analyses using
255 edgeR v.3.42.4 (Robinson *et al.* 2010) and normalized the data using the scaling factor method
256 (Anders and Huber 2010).

257 We qualitatively assessed cell population purity both by visual inspection during cell
258 sorting and following sequencing by assessing the expression of a panel of marker genes
259 specific to the four cell populations targeted by our FACS protocol and present in only a single
260 copy in the *P. sungorus* annotation. Spermatogonia markers included *Dmrt1* (Raymond *et al.*
261 2000) and *Hells* (Green *et al.* 2018). Leptotene/zygotene markers included *Ccnb1ip1* and
262 *Adad2* (Hermann *et al.* 2018). Diplotene was characterized by *Aurka* and *Tank* expression
263 (Murat *et al.* 2023) and round spermatids by *Cabyr* and *Acrv1* expression (Green *et al.* 2018).
264 To estimate relative purity, we compared mean marker gene expression across replicates for a
265 given cell population for both parent species. A cell population was considered qualitatively
266 pure if it had higher marker gene expression than other populations isolated by our FACS
267 protocol and if X-linked gene expression matched the expected regulatory dynamics (*i.e.,*
268 active vs. silenced (MSCI) vs. repressed (PSCR); Handel 2004; Namekawa *et al.* 2006). We
269 examined expression patterns across cell populations for all genes, autosomal genes, and X-

linked genes using MDS plots generated with the plotMDS function in limma v.3.56.2 (Ritchie *et al.* 2015) and heatmaps using ComplexHeatmap v.2.16.0 (Gu *et al.* 2016). MDS plots used the top 500 genes with the largest fold change difference between samples.

Differential gene expression analysis

We assessed differential gene expression by contrasting hybrids and each parent species for all cell populations. We fit the expression data for dwarf hamsters and house mice separately with negative binomial generalized linear models with Cox-Reid tagwise dispersion estimates and adjusted P-values to a false discovery rate (FDR) of 5% (Benjamini and Hochberg 1995). We quantified the biological coefficient of variation (BCV), a metric representing the variation in gene expression among replicates (McCarthy *et al.* 2012), for each dataset. Additionally, we calculated the BCV of just parental males or hybrid samples for each species for the first three cell populations to examine whether dwarf hamster hybrids exhibited more variability in expression than house mouse hybrids and parental dwarf hamsters. For our differential expression analyses, we contrasted expression between hybrids and each parent so that a positive log fold-change (logFC) indicated overexpression in sterile males and implemented a logFC cutoff of 1.25. We then categorized differentially expressed (DE) genes into one of four categories: DE relative to only one parent species, DE relative to both parent species but with intermediate expression (intermediate), and DE relative to both parent species but outside of the range of either parent species (transgressive; Figure S2 in File S1). Unless otherwise specified, results discussed in the main text are restricted to transgressive DE genes and are presented with the logFC from the contrast of the hybrid offspring to the parent with the same X chromosome (*P. campbelli* for dwarf hamster F1 hybrids and *M. m. musculus* for house mouse F1 hybrids). Transgressive DE genes have similar logFC values regardless of which parent is used as the contrast, but figures depicting the logFC between F1 hybrids and

295 *P. sungorus* or *M. m. domesticus* are provided in supplementary material. We also assessed
296 differential expression between parent species/strains (parental DE) by contrasting expression
297 between parents sharing the same X chromosome as hybrids (*i.e., M. m. musculus* and *P.*
298 *campbelli*) with parents with the alternate X chromosome (*i.e., M. m. domesticus* and *P.*
299 *sungorus*) so that a positive log fold-change indicated overexpression in parents with the same
300 X chromosome as hybrids and implemented a logFC cutoff of 1.25.

301 We tested for significant differences in the number of under and overexpressed
302 transgressive DE genes within a stage for both house mouse and hamster hybrids using X^2
303 tests with chisq.tests in R and used FDR correction for multiple comparisons. We also tested
304 for differences in the magnitude of misexpression between mouse and hamster hybrids for
305 each stage by comparing the distributions of logFC of transgressive DE genes between hybrids
306 and parent species using Wilcoxon signed-rank tests and FDR correction. To characterize
307 hybrid diplotene expression in both house mice and dwarf hamsters, we used two approaches.
308 First, we calculated Pearson's correlation coefficient *(r)* between average normalized hybrid
309 diplotene expression and the average normalized expression in each parental cell type. We
310 corrected p-values for each correlation with FDR. We generated bootstrap values for each
311 correlation coefficient by randomly sampling the expression matrices with replacement for
312 each sample type for 1000 replicates. Second, we compared the gene sets that escaped MSCI
313 in each species with gene sets that characterize stage-specific expression in parent species.
314 For this analysis, we defined sets of overexpressed X-linked diplotene genes as genes with
315 expression (normalized FPKM) in hybrids that was in the top 10% of X-linked genes in parental
316 diplotene samples (*i.e.,* genes that normally escape MSCI). We then compared these sets of
317 overexpressed hybrid diplotene genes to genes “induced” in each parental stage for each
318 species. We used gProfiler2 v.0.2.3 (Kolberg *et al.* 2020) in R to perform gene ontology (GO)
319 analysis to identify GO terms overrepresented in hybrid transgressive DE genes sets for each

320 cell population. We only included *P. sungorus* genes associated with mouse orthologs in our
321 GO analysis (as established by Moore *et al.* 2022), and for our background gene lists, we used
322 *P. sungorus* genes associated with mouse orthologs that were "expressed" in hybrids and both
323 parent species in a given stage. We retained only Biological Process GO terms with an FDR
324 below 0.05 and ran gProfiler2 both with and without the highlight option, a two-stage algorithm
325 for reducing resulting GO terms by grouping significant terms into sub-ontologies and then
326 identifying the gene sets that give rise to other significant functions (Kolberg *et al.* 2020). To
327 test whether specific chromosomes were enriched or depleted for transgressive DE genes for a
328 given stage, we performed hypergeometric tests on the number of transgressive DE genes on
329 a given chromosome with phyper and adjusted P-values to an FDR of 5%. We also assessed
330 overlap in specific transgressive DE genes within stages between house mice and dwarf
331 hamsters. We estimated whether overlap was more or less than expected by chance and
332 whether overlapping genes were preferentially located on the X chromosome using
333 hypergeometric tests and performed GO enrichment on overlapping genes. For all
334 hypergeometric tests, we defined the background sets of genes as those with non-zero logFC
335 values in both differential expression comparisons between hybrids and each parent for a
336 given spermatogenic stage.
337

338 **Characterizing the behavior of PAR genes in dwarf hamsters**

339 We sought to characterize the regulatory behavior of PAR genes in dwarf hamster
340 parent species and hybrids to determine if (1) PAR genes are normally silenced in parent
341 species (consistent with an extension of MSCI to the PAR) and (2) if PAR genes were
342 overexpressed in hybrids (consistent with disrupted MSCI in the PAR of hybrids). The PAR on
343 the *P. sungorus* X chromosome is on the distal arm of the X chromosome from around
344 115,350,000-119,112,095 bp (Moore *et al.* 2022). There are 15 annotated *P. sungorus* genes in

345 this region (Table S3 in File S1), which is comparable to the latest PAR assembly in C57BL/6J
346 house mice (Kasahara *et al.* 2022). Six of these are orthologous to annotated genes in mice
347 (*Tppp2*, *Gprin1*, *Ndrg2*, *Kcnip4*, *Ndrg2*, and *Hs6st3*), but they are not located in the mouse PAR
348 (Kasahara *et al.* 2022). Only seven of the annotated genes in the PAR were expressed in more
349 than three replicates across all samples (Psun_G000022875, Psun_G000022880,
350 Psun_G000022883, Psun_G000022886, *Tppp2*, *Gprin1*, and *Ndrg2*). For these genes, we
351 assessed whether these genes were consistently expressed or silenced in parent species in
352 any cell population and whether any genes were differentially expressed between hybrids and
353 either species.

354 **RESULTS**

355 **Impaired sperm production in hybrid male dwarf hamsters**

356 We first established the extent of hybrid male sterility in dwarf hamsters by comparing
357 reproductive phenotypes for *P. campbelli*, *P. sungorus*, and F1 hybrid males (Figure 1; Table
358 S1 in File S1). *Phodopus sungorus* males had smaller testes and seminal vesicles than *P.*
359 *campbelli* males (Dunn's Test relative testes weight $p < 0.001$; relative seminal vesicle weight p
360 $= 0.0061$; Figure 1). These differences are qualitatively consistent across independent
361 laboratory colonies (Ishishita *et al.* 2015; Bikchurina *et al.* 2018) and likely reflect species-
362 specific differences between *P. campbelli* and *P. sungorus*. *Phodopus sungorus* males also
363 had lower nucleotide diversity ($\pi = 0.00013$) than *P. campbelli* males ($\pi = 0.00045$) and both
364 house mouse parental crosses between fully inbred mouse strains (*M. m. musculus* $\pi =$
365 0.00029; *M. m. domesticus* π 0.00017; Figure S3 in File S1), which could contribute to
366 depression of male fertility within this highly inbred laboratory colony (Brekke *et al.* 2018).
367 Nucleotide divergence between parental dwarf hamster species was elevated relative to house
368 mice ($d_{xy} = 0.0020$ vs. 0.0010), consistent with reported older divergence time estimates for

dwarf hamsters (Neumann *et al.* 2006). However, these dwarf hamster species did not differ in normalized sperm counts (p = 0.071) or in sperm motility (p = 0.12). The F1 hybrid males exhibited extreme reproductive defects relative to *P. campbelli* (Figure 1). Hybrid males had smaller testes (p < 0.001) and seminal vesicles (p < 0.001) than male *P. campbelli* hamsters, and importantly, produced almost no mature spermatozoa. In the one instance where a hybrid male produced a single mature spermatozoon, it was non-motile, indicating severe reproductive impairment in hybrid males. Overall, our results confirmed previous reports of reduced fertility in hybrid male dwarf hamsters (Ishishita *et al.* 2015; Bikchurina *et al.* 2018).

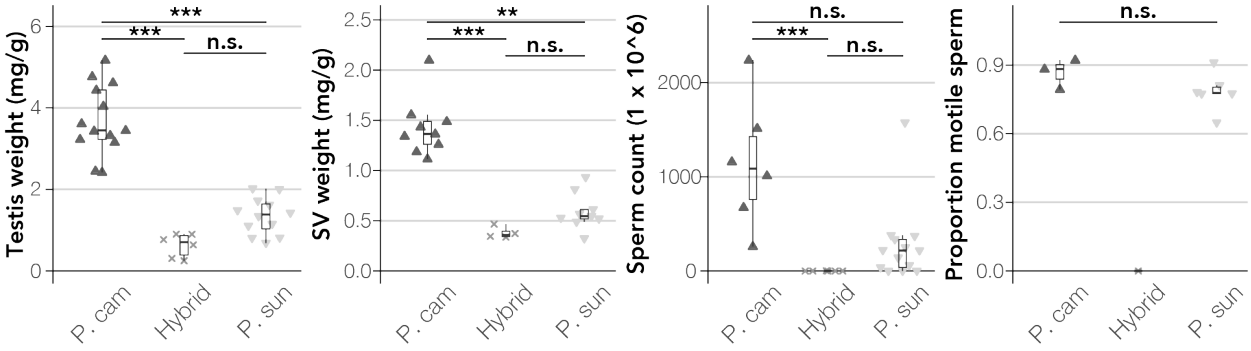

Figure 1. Evidence of some hybrid male sterility in dwarf hamsters. We assessed paired testes weight and paired seminal vesicle weight (SV; both normalized by body weight), sperm count, and proportion of motile sperm for *P. sungorus*, *P. campbelli*, and F1 hybrids. Whiskers extend to either the largest or smallest value or no further than 1.5 times the interquartile range, and *** indicates p < 0.001, ** indicates p < 0.01, and n.s. indicates non-significant difference between means at p > 0.05 using a post-hoc Dunn's test with FDR correction. Upwards-pointing triangles (▲) indicate *P. campbelli*, downwards-pointing triangles (▼) indicate *P. sungorus*, and crosses (✖) indicate F1 hybrids.

388 **Cell type-specific gene expression across spermatogenesis**

389 To characterize cell type-specific gene expression, we used FACS to isolate enriched
390 cell populations from each fertile parent species and their sterile F1 hybrids across four stages
391 of spermatogenesis. The four targeted populations included: spermatogonia (mitotic precursor
392 cells), leptotene/zygotene spermatocytes (meiotic cells before MSCI), diplotene spermatocytes
393 (meiotic cells after MSCI), and round spermatids (postmeiotic cells). We were unable to isolate
394 round spermatids from the F1 hybrids, which was consistent with the lack of mature
395 spermatozoa present in the cauda epididymis extractions (Figure 1). We sequenced RNA from
396 each cell population for *P. campbelli* (spermatogonia n = 4, leptotene/zygotene n = 5, diplotene
397 n = 5, and round spermatids n = 4; Table S2 in File S1), *P. sungorus* (spermatogonia n = 4,
398 leptotene/zygotene n = 4, diplotene n = 5, and round spermatids n = 3), and F1 hybrid males (
399 *P. campbelli* ♀ x *P. sungorus* ♂; spermatogonia n = 4, leptotene/zygotene n = 4, diplotene n =
400 4). We compared our hamster expression data to an analogous cell type-specific RNASeq
401 dataset from two species of house mice, *Mus musculus musculus* and *M. m. domesticus*, and
402 their sterile F1 hybrids (n = 3 for all cell populations in each cross; Larson *et al.* 2017).

403 We used two approaches to qualitatively evaluate the purity of spermatogonia,
404 leptotene/zygotene spermatocytes, diplotene spermatocytes, and round spermatids isolated
405 from males from both parental species: (1) we quantified the relative expression of a panel of
406 cell population marker genes, and (2) we characterized the expression patterns of the sex
407 chromosomes across development. We found that our candidate marker genes had the
408 highest expression in their expected cell population for all stages except leptotene/zygotene
409 (Figures S4 and S5 in File S1), indicating high purity of spermatogonia, diplotene
410 spermatocytes, and round spermatids. Leptotene/zygotene markers did not have the highest
411 expression in leptotene/zygotene samples (except for *Ccnb1ip1*), potentially indicating lower
412 purity of this cell population. Nonetheless, the patterns of X chromosome expression in fertile

413 parents were consistent with expectations across this developmental timeline: the X
414 chromosome had active expression in spermatogonia and leptotene/zygotene cells, was
415 inactivated in diplotene cells consistent with MSCI, and was partially inactivated in round
416 spermatids, consistent with PSCR (Figure 2; Namekawa *et al.* 2006), indicating successful
417 isolation of these cell populations.

418 When we examined overall expression differences within dwarf hamsters and within
419 house mice, we found that samples clustered primarily by cell population on MDS1 and 2
420 (Figure 3), then by cross/strain when cell populations were examined separately (Figures S6
421 and S7 in File S1). Within all cell populations across both systems, hybrids showed
422 intermediate overall expression patterns to parent species (Figures S6 and S7 in File S1).
423 However, in dwarf hamsters but not house mice, spermatogonia and leptotene/zygotene
424 samples overlap rather than forming distinct clusters (Figure 3). Further, the expression profiles
425 of hybrid diplotene cell populations ranged from clustering with parental leptotene/zygotene to
426 parental diplotene cell populations, which contrasted with what we observed in house mice
427 where hybrid diplotene cell populations clustered distinctly with parental diplotene cell
428 populations (Figure 3). Overall, our results indicate that we successfully isolated cell
429 populations in dwarf hamsters that span key stages of spermatogenesis.

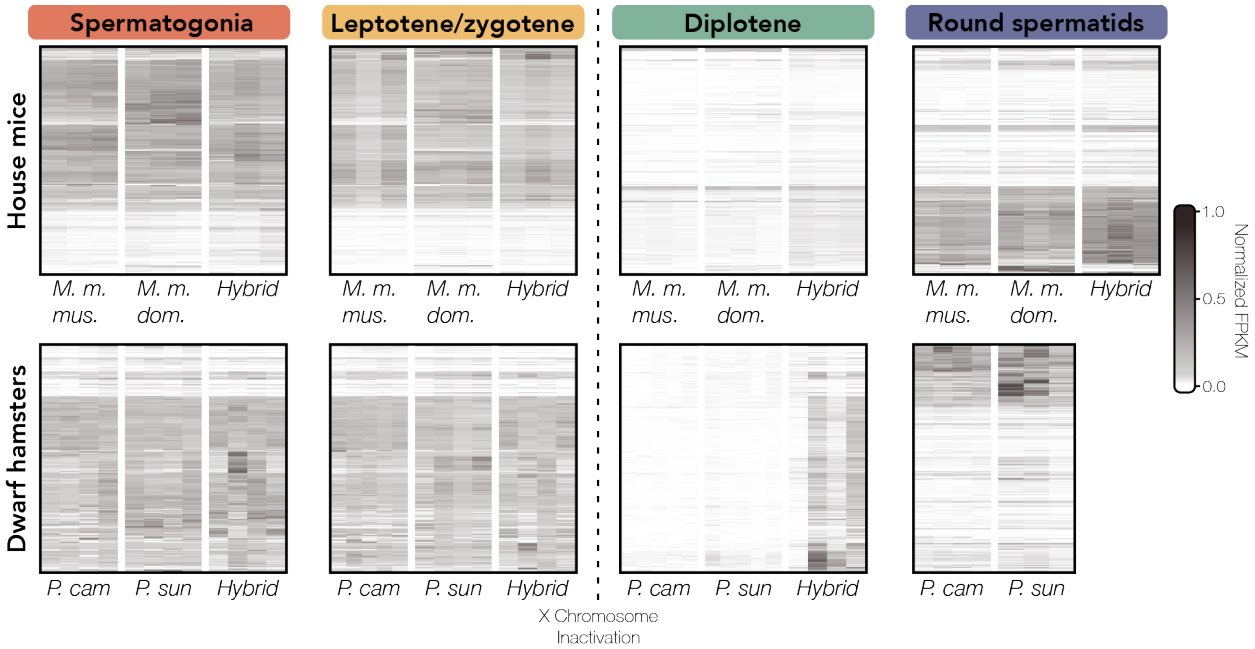

Figure 2. Overexpression of X-linked genes in diplotene spermatocytes in both house mouse and dwarf hamster hybrids. Heatmap of X-linked gene expression in house mice (upper panel) and dwarf hamsters (lower panel) plotted as normalized FPKM values that are hierarchically clustered using Euclidean distance. Each column represents a different individual, each row represents a gene, and darker colors indicate higher expression. The heatmap was generated with the R package ComplexHeatmap v.2.12.0 (Gu et al. 2016). Note, hybrid dwarf hamsters do not produce mature spermatozoa, and accordingly, we were unable to isolate round spermatids.

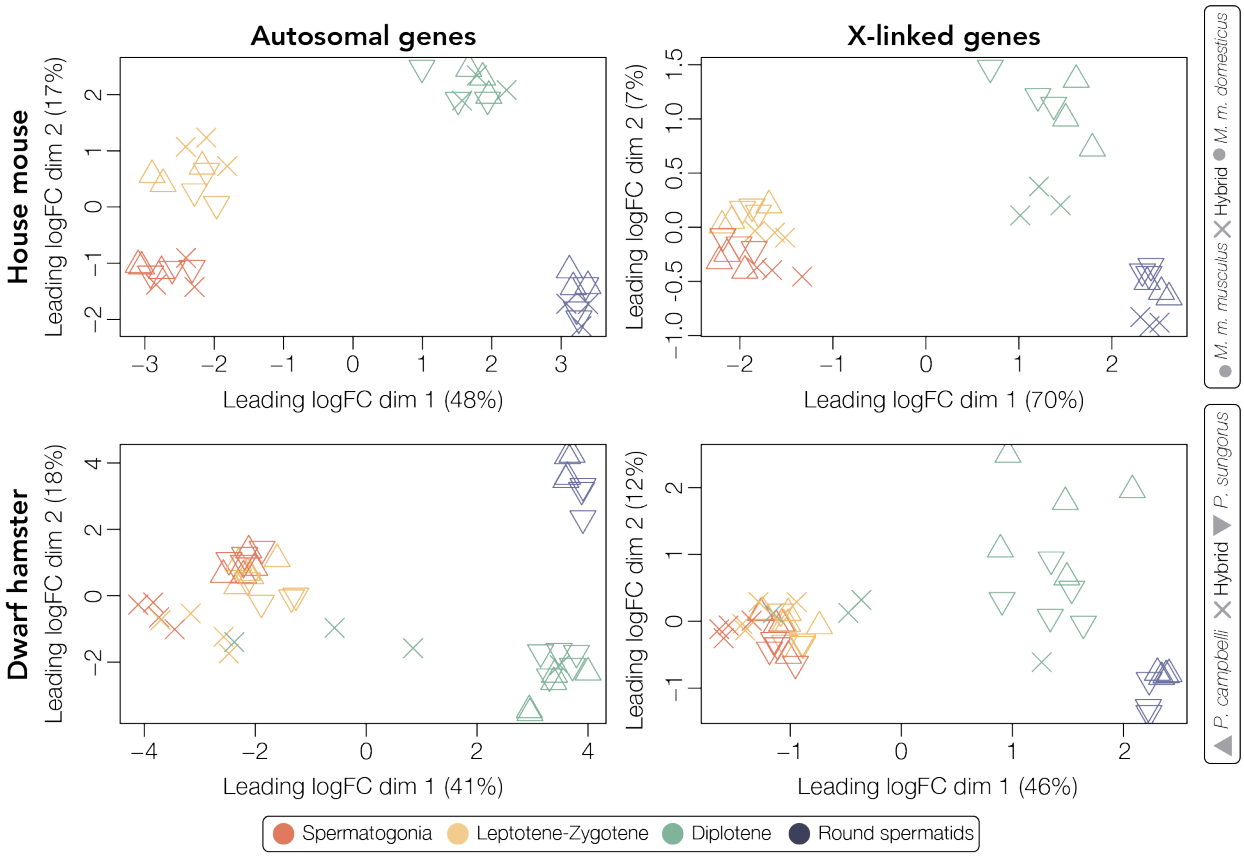

Figure 3. Hybrid gene expression profiles cluster by parental spermatogenic cell population in house mice but not dwarf hamsters. Multidimensional scaling (MDS) plots of distances among house mouse (upper panels) and dwarf hamster (lower panels) samples for expressed autosomal (left) and X-linked (right) genes. Distances are calculated as the root-mean-square deviation (Euclidean distance) of log2 fold changes among the top 500 genes that distinguish each sample. Each strain or cross is indicated by a symbol, and samples are colored by cell population.

Disrupted transcription early in spermatogenesis in dwarf hamsters

We sought to characterize which expression phenotypes were associated with sterile hybrids in both house mice and dwarf hamsters. We first investigated whether differential gene expression in hybrids tended towards intermediate or transgressive expression, and then

452 within transgressive DE genes, whether misexpression tends towards up- or downregulation in
453 hybrids compared to parents. Differential gene expression in mouse hybrids had a slight bias
454 towards transgressive expression except in round spermatids (percentage of transgressive DE
455 genes: SP: 72.0%, LZ: 62.7%, DIP: 60.8%, and RS: 24.9%; Figures 4b and S2 in File S1), while
456 almost all differential expression in dwarf hamster hybrids was transgressive (percentage of
457 transgressive DE genes: SP: 99.2%, LZ: 98.0%, and DIP: 97.1). For transgressive DE genes,
458 autosomal misexpression in hybrid house mice was biased towards upregulation across
459 spermatogenesis (mean logFC of spermatogonia autosomal transgressive DE genes: +1.90/ X^2:
460 $p < 0.001$; leptotene/zygotene: +1.33/ X^2: $p < 0.001$; diplotene: +0.47/ X^2: $p < 0.001$; Figures 4c
461 and S8 in File S1), as was X-linked misexpression (spermatogonia mean logFC: +1.98 / X^2: $p <$
462 0.001; leptotene/zygotene: +2.50/ X^2: $p < 0.001$; diplotene: +2.78/ X^2: $p < 0.001$). In contrast,
463 we found that the direction of misexpression in dwarf hamster hybrids was cell type-specific.
464 Autosomal transgressive DE genes in dwarf hamster hybrids were overwhelmingly
465 downregulated in both early stages of spermatogenesis, especially in comparison to house
466 mice (mean logFC of spermatogonia autosomal transgressive DE genes: -4.38/ X^2: $p < 0.001$;
467 leptotene/zygotene: -4.67/ X^2: $p < 0.001$; Figure 4d) but upregulated in diplotene (average
468 logFC = +4.67/ X^2: $p < 0.001$; Figures 4d and S8 in File S1). When comparing both X-linked and
469 autosomal expression in dwarf hamsters, we found similar patterns: almost all X-linked
470 transgressive DE genes in the first two stages of spermatogenesis were exclusively
471 downregulated (spermatogonia mean logFC = -6.57/ X^2: $p < 0.001$; leptotene/zygotene: -6.73/
472 X^2: $p < 0.001$), but misexpression was biased towards upregulation in diplotene (mean logFC:
473 5.70/ X^2: $p < 0.001$).

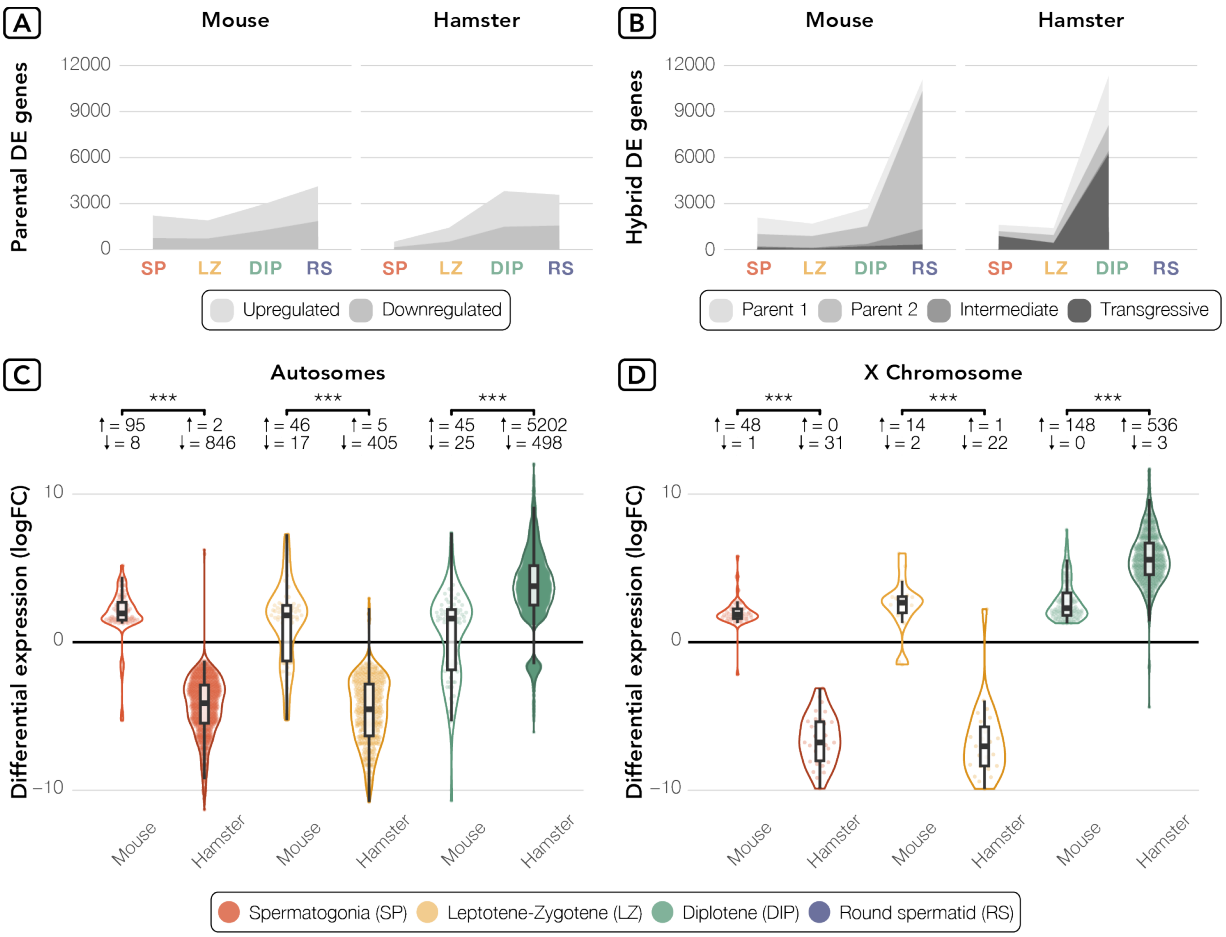

Figure 4. House mice and dwarf hamster hybrids have opposite patterns of disrupted regulation early in spermatogenesis. a) Up- and down-regulated DE genes between parent species for house mice (left; *M. m. musculus* vs. *M. m. domesticus*) and dwarf hamsters (right; *P. sungorus* vs. *P. campbelli*). b) Counts of DE genes between hybrids and one parent species (two lightest shades of gray where Parent 1 was either *M. m. musculus or P. sungorus* and parent 2 was either *M. m. domesticus* or *P. campbelli)* or between hybrids and both parents (two darker shades of gray) that showed either intermediate or transgressive expression. c) Transgressive DE genes in house mouse and dwarf hamster hybrids for autosomal genes where the logFC represents hybrid expression relative to *M. m. musculus* or *P. campbelli,* respectively, and d) transgressive DE gene expression for X-linked genes. Results are displayed for autosomes (left) and the X chromosome (right). *** indicates $p < 0.001$ for

486 pairwise comparisons from Wilcoxon signed-rank tests after FDR correction. Whiskers extend
487 to either the largest or smallest value or no further than 1.5 times the interquartile range. The
488 number of up and downregulated transgressive DE genes in hybrids are listed next to arrows
489 indicating direction of differential expression.
490
491 Second, we investigated how developmental stage influenced the extent of hybrid
492 misexpression. In both systems, the number of DE genes between parent species increased
493 with the progression of spermatogenesis, consistent with less constraint on gene expression
494 levels as spermatogenesis progresses (Figure 4a; Kopania *et al.* 2022a; Murat *et al.* 2023).
495 Similarly, transgressive misexpression in both hybrid dwarf hamsters and house mice
496 increased with the progression of spermatogenesis, though to a greater extent in dwarf
497 hamsters (Figure 4b). While both parental DE genes and transgressive hybrid DE genes
498 increased with the progression of spermatogenesis, parental DE genes initially exceeded the
499 number of transgressive hybrid DE genes in hybrids in spermatogonia and leptotene/zygotene
500 spermatocytes. However, in diplotene spermatocytes, transgressive hybrid differential
501 expression surpassed parental differential expression in both house mice and dwarf hamsters.
502 We also found a much greater genome-wide disruption of expression in diplotene cell
503 populations of hybrid dwarf hamsters than in hybrid house mice (Figures 4c, 4d, and S8-S10 in
504 File S1), indicating more widespread regulatory disruption. We then compared transgressive
505 DE genes between house mice and dwarf hamster hybrids across all three stages and found
506 that the number of shared transgressive DE genes did not differ from the number expected by
507 chance in early spermatogenesis (spermatogonia = 3 genes, hypergeometric test $p = 0.98$;
508 leptotene/zygotene = 2 genes, $p = 0.59$; Table S4 in File S1). However, the number of shared
509 transgressive DE genes did exceed the number expected by chance in diplotene cell
510 populations ($n = 68$; $p < 0.001$), and these shared genes were preferentially located on the X

511 chromosome (61/68; $p < 0.001$). Additionally, these sets of shared transgressive DE genes
512 between house mice and dwarf hamsters were not significantly enriched for any GO terms,
513 though many play known roles in spermatogenesis, the apoptotic process, and cell
514 differentiation (Table S5 in File S1) and may be promising candidates for future functional
515 analysis. Ultimately, we found that there are similar trends in the patterns of transgressive
516 expression across stages in both systems, and although few specific genes had disrupted
517 expression in both dwarf hamster and house mouse hybrids, genes with similar patterns of
518 disrupted expression tend to be X-linked and disrupted in later stages of spermatogenesis.
519 To determine if the differences we observed in the extent of misexpression between
520 dwarf hamsters and house mice was due to greater expression variability across our dwarf
521 hamster samples, we calculated the BCV, a measurement of inter-replicate variability, for each
522 species and hybrid across the first three cell populations. Inter-replicate variability was higher
523 in dwarf hamster hybrids relative to house mouse hybrids (dwarf hamster BCV = 0.69; house
524 mice = 0.18). Additionally, nucleotide diversity within dwarf hamster hybrids was higher (π =
525 0.0012) than within house mouse hybrids (π = 0.00052; Figure S3 in File S1). However, the
526 extent of the expression variability observed in hybrids relative to the inter-replicate variability
527 of parental species differed between house mice and dwarf hamsters: dwarf hamster hybrid
528 variability was more than dwarf hamster parental samples (*P. campbelli* = 0.49; *P. sungorus* =
529 0.40), but hybrid variability was similar to parental samples for house mice (*M. m. musculus* =
530 0.19; *M. m. domesticus* = 0.22). The greater inter-replicate expression variability in dwarf
531 hamster hybrids relative to parent species suggests that the increased misexpression we see
532 in hybrids cannot be explained by greater inter-replicate variability in our dwarf hamster
533 samples alone, and it may also reflect the greater nucleotide diversity present among dwarf
534 hamster hybrids.

535 Third, we characterized whether there was a clear difference between the autosomes
536 and sex chromosomes in expression phenotype by testing whether the X chromosome was
537 enriched for transgressive DE genes in each stage for both systems. Across all stages of
538 spermatogenesis in house mice, the X chromosome was enriched for transgressive DE genes
539 between hybrids and parents (spermatogonia $p < 0.001$; leptotene/zygotene $p < 0.001$;
540 diplotene $p < 0.001$; round spermatids $p < 0.0036$; Figure S9 in File S1). In contrast,
541 misexpression in dwarf hamsters was not uniformly sex chromosome-specific across all
542 stages, as the sex chromosomes in dwarf hamsters showed no enrichment for transgressive
543 DE genes early in spermatogenesis (spermatogonia: $p = 0.21$; Figure S10 in File S1) despite X
544 chromosome enrichment in both leptotene/zygotene ($p = 0.0064$) and round spermatids ($p <$
545 0.001). However, we note that the magnitude of misexpression was greater for sex
546 chromosomes than autosomes in dwarf hamsters across all stages (Figures 4c and 4d;
547 discussed above). Only two autosomes were enriched for transgressive DE genes in dwarf
548 hamsters in any cell population: one scaffold on chromosome 5 in spermatogonia
549 (JAJQIY010003390.1; hypergeometric test; $p = 0.003$) and chromosome 11 in
550 leptotene/zygotene ($p = 0.017$; Figure S10 in File S1). Together, the subtle differences in the
551 distribution of transgressive DE genes across autosomes and the X chromosome between
552 dwarf hamster hybrids and house mouse hybrids suggest a difference in the extent of the role
553 for sex chromosome-specific disruption between systems.
554

555 **Misexpression in diplotene appears to be unrelated to disrupted MSCI in dwarf hamsters**

556 We next asked whether expression patterns indicated similar disrupted regulatory
557 processes resulting in sex chromosome-specific misexpression in both systems. In sterile
558 hybrid house mice, the mean logFC of transgressive X-linked DE genes during diplotene was
559 higher than the mean logFC of transgressive autosomal DE genes (X logFC = +2.78 in contrast

560 to autosomal logFC = +0.47; Figures 4c and 4d), consistent with disrupted MSCI (Good *et al.*
561 2010; Bhattacharyya *et al.* 2013; Campbell *et al.* 2013; Turner and Harr 2014; Larson *et al.*
562 2017, 2022). In sterile dwarf hamster hybrids, we also found elevated mean logFC of
563 transgressive X-linked DE genes relative to autosomal genes (X logFC = +5.70 in contrast to
564 autosomal logFC = +3.69), but the extent of X chromosome overexpression, as measured by
565 logFC of X-linked transgressive DE genes, was greater than in hybrid house mice (5.7/3.69 or
566 ~1.5x higher; Figures 2, 4c, and 4d). There was also more variability in the extent of
567 overexpression of X-linked genes in hybrid dwarf hamsters compared to normal parental X-
568 linked expression during diplotene (relative overexpression = 18.5 +/- 6.8) than for
569 overexpression of X-linked genes in hybrid house mice compared to normal parental X-linked
570 expression in diplotene (relative overexpression = 1.75 +/- 0.09; Figures 2 and S11 in File S1).
571 Strikingly, some hybrid male dwarf hamsters had an almost completely silenced X
572 chromosome, while others had an almost completely transcriptionally-activated X chromosome
573 (Figure 2).
574 Despite overexpression of the X chromosome during diplotene in hybrid dwarf
575 hamsters, the overall expression phenotype, including the identity and the extent of
576 misexpression of overexpressed genes, appeared to fundamentally differ between house
577 mouse and dwarf hamster hybrids (Figures 2 and 5a-5c). We established these differences in
578 X-linked overexpression using two approaches. First, we tested which parental cell types had
579 the highest expression correlation with hybrid diplotene cell types for both X-linked and
580 autosomal genes. In mice, the expression profile of X-linked genes in hybrids during diplotene
581 was most positively correlated with the expression profile of X-linked parental round spermatid
582 genes, consistent with disrupted MSCI (spermatogonia *(r)* = -0.25, $p < 0.001$;
583 leptotene/zygotene *(r)* = -0.073, $p = 0.035$; round spermatid *(r)* = 0.26, $p < 0.001$; Figures 2 and
584 5a). Autosomal diplotene genes showed no positive correlations with either spermatogonia (*r* =

585 -0.26; $p < 0.001$), leptotene/zygotene ($r = -0.032$; $p < 0.001$), or round spermatids ($r = -0.060$; p
586 < 0.001; Figure 5a). If the X-linked overexpression phenotype in dwarf hamsters was consistent
587 with disrupted MSCI, then we would also expect X-linked and autosomal expression profiles in
588 hybrid diplotene to follow the same patterns. In contrast to this prediction, hybrid dwarf
589 hamster diplotene expression profiles for both X-linked and autosomal genes had a positive
590 correlation with parental leptotene/zygotene (autosomal $(r) = 0.14$, $p < 0.001$; X-linked $(r) =$
591 0.22, $p < 0.001$) and spermatogonia (autosomal $(r) = 0.027$, $p < 0.001$; X-linked $(r) = 0.091$, $p =$
592 0.016) and a negative correlation with round spermatids (autosomal $(r) = -0.30$, $p < 0.001$; X-
593 linked $(r) = -0.31$, $p < 0.001$; Figure 5b). These striking differences in the strength and direction
594 of expression profile correlations suggest that the regulatory mechanisms underlying the
595 overexpression phenotype of X-linked genes in sterile hybrids differed between house mice
596 and dwarf hamsters.

597 This difference in pattern was further supported when we compared which sets of
598 genes were overexpressed in hybrid diplotene in dwarf hamsters and house mice. For this
599 approach, we looked at parental gene expression patterns to characterize which stages of
600 spermatogenesis all genes were normally active during and characteristic of (*i.e.,* "induced";
601 see Methods). Using this information, we then identified which X-linked genes were
602 overexpressed in hybrid diplotene (defined as genes with normalized expression in the top
603 10% of X-linked genes) and assessed which parental stages the overexpressed X-linked genes
604 were characteristic of in both systems. As in our correlation analysis, we found that in hybrid
605 house mice, the genes that were overexpressed in diplotene most closely resembled genes
606 that are normally active in round spermatids in parental mice (51.6% of genes), but that in
607 hybrid dwarf hamsters, overexpressed diplotene genes resembled spermatogonia- and
608 leptotene/zygotene-specific genes (47.6% and 41.6% respectively; Figure 5c). Because of the
609 dissimilarity in the genes that were overexpressed during diplotene in both systems, we next

610 performed gene ontology (GO) enrichment analyses on the set of transgressive DE genes in
611 hybrids to determine which biological processes could be potentially contributing to this
612 pattern. In contrast to house mice hybrids where transgressive DE genes were enriched for no
613 biological processes, the transgressive DE genes in dwarf hamster were enriched for several
614 biological processes including cell junction/extracellular matrix organization, system
615 development, inflammatory response, and apoptotic process which together point to
616 widespread disruption of numerous processes necessary for normal male fertility (highlighted
617 terms presented in Figure 5d and the full lists in Tables S6-S8 in File S1). Collectively, these
618 results suggest that the X-linked overexpression phenotype in sterile hybrid dwarf hamsters is
619 inconsistent with disrupted MSCI and is possibly related to a stalling and breakdown of
620 spermatogenesis between leptotene/zygotene and diplotene during Prophase I.

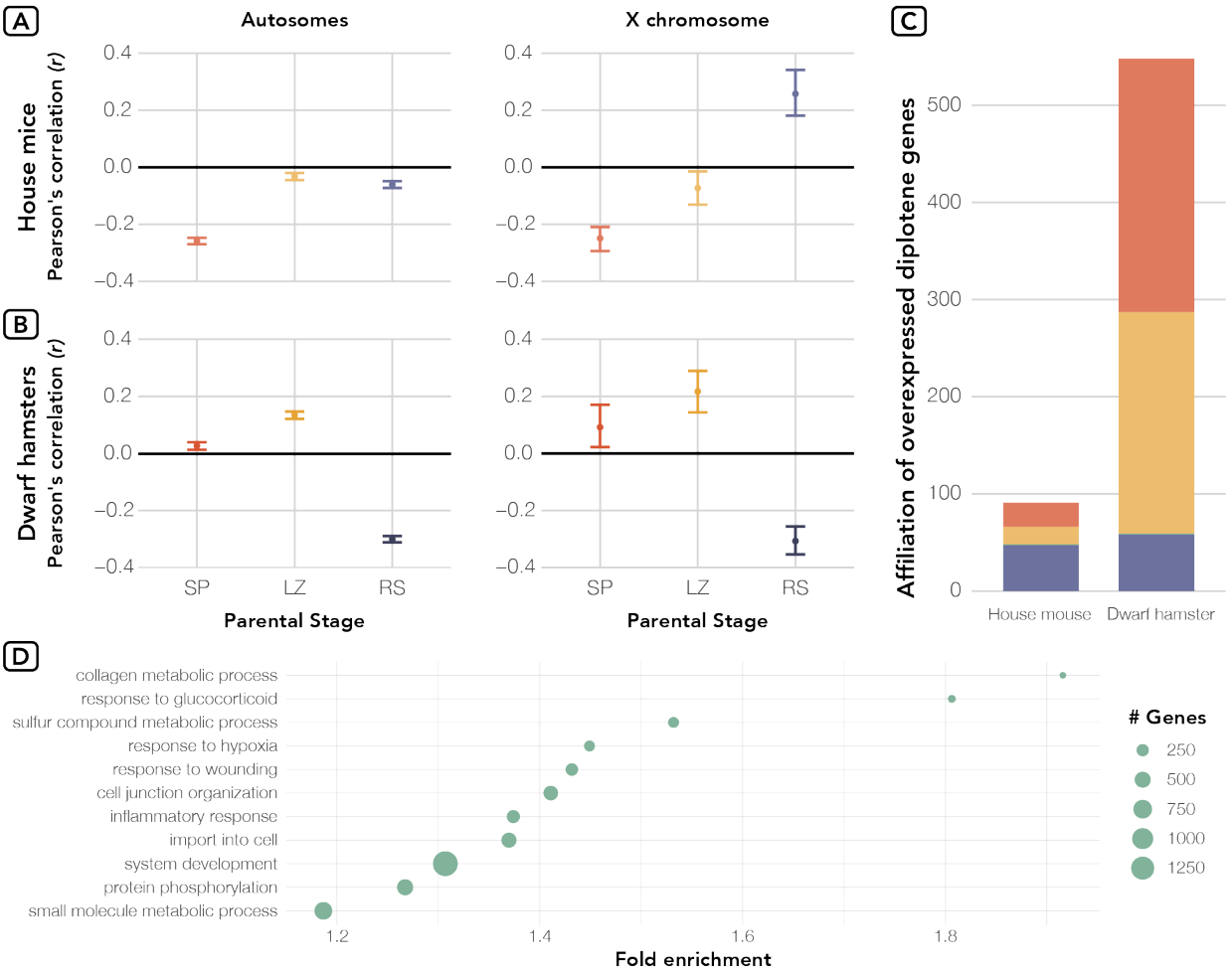

Figure 5. Spermatogenesis in hybrid dwarf hamsters appears to stall after leptotene/ zygotene. a) We calculated the Pearson's correlation coefficient *(r)* between mean hybrid diplotene expression and the mean expression for each parental cell type for both house mice and b) dwarf hamsters. Correlation coefficients were calculated for both autosomal (left panels) and X-linked (right panels) genes. We then generated bootstrap values by randomly sampling the expression matrices for 1000 replicates. All correlation coefficients were significantly different from zero ($p < 0.05$) after FDR correction. c) Classification of X-linked overexpressed genes in diplotene cell populations of hybrid mice and dwarf hamsters by parental stage in which genes are induced. Genes are colored by cell type (red = spermatogonia, yellow = leptotene/zygotene, green = diplotene, and blue = round spermatids). d) Select enriched

632 Biological Process GO terms (ranked by FDR) for transgressive DE genes between hybrid
633 dwarf hamsters and *P. campbelli* in diplotene spermatocytes. Included terms shown are the
634 result of the highlight function within gProfiler2 which collapses GO terms in a two-step
635 clustering algorithm (Kolberg *et al.* 2020). Point size corresponds to the number of genes
636 belonging to each GO term, and terms are plotted by the fold enrichment of the GO term in the
637 dataset relative to the provided gene backgrounds.
638

639 **PAR expression was not disrupted in sterile hybrid dwarf hamsters**

640 Finally, we tested the hypothesis that hybrid sterility in dwarf hamsters may be
641 correlated with asynapsis of the X and Y chromosomes because of divergence in the
642 pseudoautosomal region (PAR) which prevents proper chromosome pairing (Bikchurina *et al.*
643 2018). The PAR is the only portion of the sex chromosomes that is able to synapse during
644 routine spermatogenesis, and PAR genes are assumed to escape silencing by MSCI
645 (Raudsepp and Chowdhary 2015). However, because XY asynapsis is common in dwarf
646 hamster hybrids, Bikchurina et al. (2018) hypothesized that MSCI may extend to the PAR of
647 hybrid male dwarf hamsters, resulting in the silencing of PAR genes in hybrids that may be
648 critical to meiosis (Figure 6a). To test this hypothesis, we compared the expression of genes
649 located in the dwarf hamster PAR (Moore et al. 2022) between parental dwarf hamster species
650 and hybrid offspring across the timeline of spermatogenesis. Specifically, we hypothesized that
651 if XY asynapsis results in an extension of MSCI to the PAR in hybrid dwarf hamsters, then
652 hybrids should have similar PAR gene expression to parents early in meiosis before
653 homologous chromosome synapse during pachytene. This should be followed by the silencing
654 of PAR genes in hybrids, but not parent species, during diplotene. If XY asynapsis does not
655 alter the regulation of the PAR in hybrids, then we may see two possible patterns. First, if all
656 PAR genes are critical to the later stages of spermatogenesis, then PAR genes in both hybrids

657 and parents should be uniformly expressed in diplotene. Alternatively, if PAR genes are not
658 critical to the later stages of spermatogenesis, then hybrids and parent species should have
659 similar PAR gene expression, and not all PAR genes may be expressed during diplotene.
660

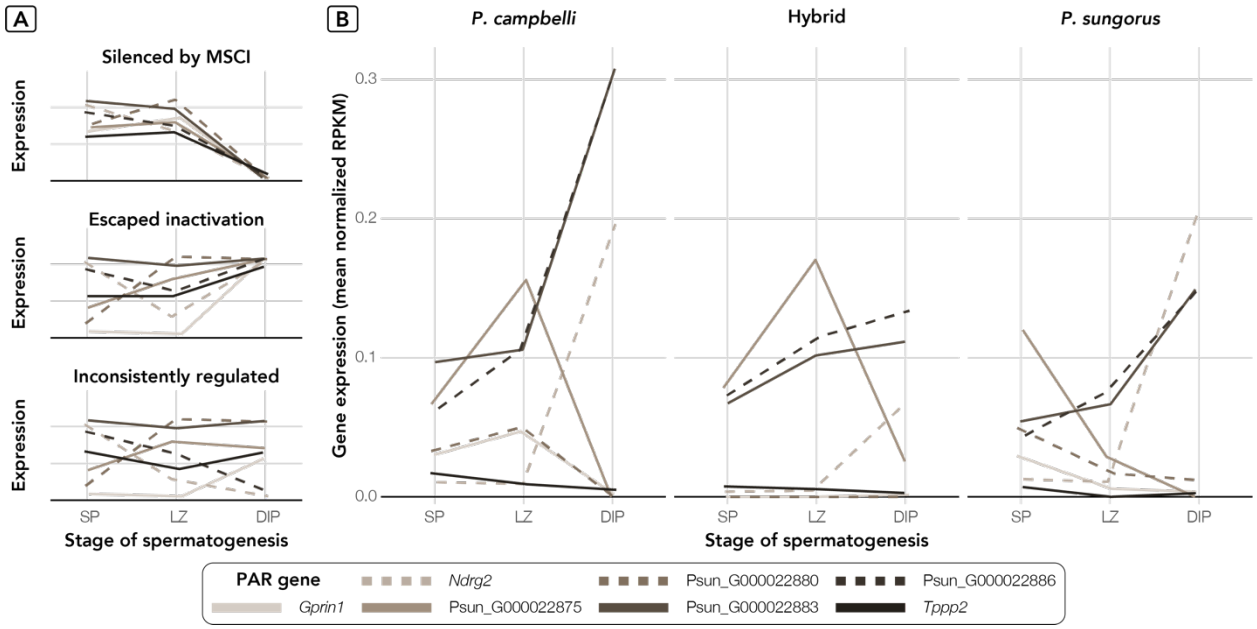

661

662 **Figure 6. PAR gene expression is not disrupted during spermatogenesis in hybrid dwarf**
663 **hamsters.** a) Hypothesized types of PAR gene expression across spermatogenesis. If MSCI
664 extends to the entire X chromosome, then PAR genes would show some level of expression
665 early in spermatogenesis which would then drop to zero in diplotene when MSCI occurs. If the
666 PAR escapes silencing by MSCI and if PAR genes are critical to spermatogenesis, then we
667 would expect PAR genes to be uniformly expressed in diplotene when the rest of the X
668 chromosome is silenced. Finally, if the PAR escapes silencing by MSCI but all PAR genes are
669 not critical to spermatogenesis, then we would expect some PAR genes to be expressed and
670 some to be not expressed in diplotene. b) Observed patterns of PAR gene expression (as mean
671 normalized RPKM across individuals) in parental species and hybrid dwarf hamsters for all PAR

genes (indicated by line type and color) across spermatogenesis (SP = spermatogonia, LZ = leptotene/zygotene^{-}, and DIP = diplotene).

We did not find evidence supporting PAR-wide silencing in dwarf hamster hybrids during diplotene suggesting that MSCI is not extended to the PAR in dwarf hamster hybrids because of XY asynapsis (Figure 6b). Furthermore, we do not see PAR-wide expression of genes during diplotene in hybrids or parents, indicating that not all PAR genes are critical to the progression of spermatogenesis in dwarf hamsters. In general, most PAR gene expression followed similar trends between hybrids and parent species. Two PAR genes were differentially expressed between hybrids and *P. campbelli* during diplotene (*Ndrg2* and Psun_G000022883; Table S3 in File S1), but these genes were still expressed in hybrids. Further, an association between PAR misregulation during the early stages of spermatogenesis and hybrid male sterility also seems unlikely as only one gene, *Gprin1*, showed transgressive differential expression in early meiosis between both parent species and hybrids (Table S3 in File S1). Thus, based on the current annotation of the PAR in *P. sungorus*, we currently find no direct evidence linking improper silencing of PAR genes to hybrid male sterility in dwarf hamsters.

DISCUSSION

We used a comparative approach to understand common gene expression phenotypes associated with hybrid male sterility in two divergent rodent crosses. We characterized the asymmetry in the expression patterns of transgressive genes, how misexpression changed over developmental timelines, and how the X chromosome and autosomes differed in both of these aspects. We found that while there were similarities in hybrid expression phenotypes in house mice and dwarf hamsters, there were also differences in the timing and chromosomal

distribution of disrupted gene expression that point towards different underlying mechanisms behind hybrid male sterility.

Asymmetry and developmental timing of misexpression in hybrids

We first investigated patterns of transgressive gene misexpression in sterile male hybrids. Studies of transgressive misexpression in sterile or inviable hybrids have often focused on whether hybrid expression is biased towards over or underexpression, with the hypothesis that expression may be biased towards overexpression if hybrid incompatibilities disrupt repressive gene regulatory elements (Meiklejohn *et al.* 2014; Barreto *et al.* 2015; Larson *et al.* 2017). In house mice, there is strong support for overexpression of both autosomal and X-linked genes in sterile F1 hybrids (Mack *et al.* 2016; Larson *et al.* 2017, 2022; Hunnicutt *et al.* 2022). Surprisingly, we found that in dwarf hamster hybrids, there was nearly uniform downregulation of transgressive DE genes in mitotic and early meiotic cell populations, suggesting that a loss of regulatory repression is not an inevitable outcome of hybrid genomes. Hybrid house mice expression is also more similar to the parent with the same X chromosome, *M. m. musculus,* than to the parent with a different X chromosome, *M. m. domesticus* (Figure 4b and S2 in File S1; Larson *et al.* 2017). Further work in house mice has shown that F1 hybrid expression patterns depend on both autosomal background and sex chromosome mismatch (Kopania *et al.* 2022b). In contrast, hybrid dwarf hamsters showed similar levels of misexpression in both the *P. campbelli* and *P. sungorus* comparisons. Determining what factors shape the misexpression of parental alleles is a fruitful area of future research.

Asymmetric patterns of misexpression have been found in many hybrids, including underexpression in sterile *Drosophila* hybrids (Michalak and Noor 2003; Haerty and Singh 2006; Llopart 2012) and sterile introgression lines of tomato (Guerrero *et al.* 2016) and *Drosophila* (Meiklejohn *et al.* 2014), but overexpression has also been found in other sterile

720 hybrids (Llopart 2012; Davis *et al.* 2015). In many of these studies, patterns of misexpression
721 may be complicated by differences in cell composition or differences in the developmental
722 timeline of sterile hybrids and their parents (Good *et al.* 2010; Wei *et al.* 2014; Montgomery and
723 Mank 2016; Kerwin and Sweigart 2020; Hunnicutt *et al.* 2022). The variation we and others
724 have found in hybrid expression phenotypes suggests that the mechanisms of disrupted
725 expression are complex, even within groups with relatively shallow divergence times, such as
726 rodents, and we need more data from diverse hybrid sterility systems to begin to understand
727 common drivers of transgressive hybrid misexpression.

728 The downregulation we observed in early spermatogenesis in hybrid dwarf hamsters
729 could be due to impaired transcription factor binding with promoter or enhancer elements (Oka
730 *et al.* 2014; Guerrero *et al.* 2016) or disrupted epigenetic silencing. Disruption of epigenetic
731 regulation of gene expression has been increasingly linked to hybrid dysfunction in plants
732 (Shivaprasad *et al.* 2012; Lafon-Placette and Köhler 2015; Zhu *et al.* 2017), especially
733 polyploids (Paun *et al.* 2007), and may also contribute to hybrid male sterility in *Drosophila*
734 (Bayes and Malik 2009) and cattle x yak hybrids (Luo *et al.* 2022). At least one known
735 chromatin difference, an expansion of the heterochromatin-enriched Xp arm of the X
736 chromosome, has been documented between parental dwarf hamster species (Gamperl *et al.*
737 1977; Haaf *et al.* 1987). However, it is unknown what the functional consequences of this
738 chromatin state divergence or other diverged epigenetic regulatory mechanisms, such as
739 methylation, may be in hybrid dwarf hamster spermatogenesis, and further work is needed to
740 distinguish between potential mechanisms underlying the observed genome-wide
741 downregulation.

742 Spermatogenesis as a developmental process may be sensitive to disruption (Lifschytz
743 and Lindsley 1972; Wu and Davis 1993), but it remains an open question whether specific
744 stages of spermatogenesis, or developmental processes more broadly, may be more prone to

745 the accumulation of hybrid incompatibilities. In general, earlier developmental stages are
746 thought to be under greater pleiotropic constraint and less prone to disruption (Cutter and
747 Bundus 2020). With the progression of mouse spermatogenesis, pleiotropy decreases (as
748 approximated by increases in tissue specificity; Murat *et al.* 2023) and the rate of protein-
749 coding evolution increases (Larson *et al.* 2016; Kopania *et al.* 2022a; Murat *et al.* 2023), which
750 may make the later stages of spermatogenesis more prone to accumulating hybrid
751 incompatibilities. Indeed, we found fewer DE genes both between parent species and in sterile
752 hybrids for both dwarf hamsters and house mice during the early stages of spermatogenesis
753 than in later stages (Figures S9 and S10), and hybrid misexpression greatly exceeds parental
754 expression divergence in late spermatogenesis. When examining transgressive DE genes
755 shared between analogous cell types in dwarf hamster and house mouse hybrids, we found
756 that there were similar or fewer shared genes than expected by chance during early
757 spermatogenesis but more shared genes than expected by chance, especially on the X
758 chromosome, in later spermatogenesis, suggesting that disrupted expression of shared genes
759 of large effect during early spermatogenesis is unlikely to be responsible for the repeated
760 evolution of hybrid male sterility in these species.

761 Despite general similarities in patterns of misexpression across spermatogenesis in
762 hybrids, studies in house mice suggest that early spermatogenesis may be tolerant of some
763 misregulation as low levels of gene misexpression in early meiotic stages does not always
764 correlate with a complete cessation of sperm development (Oka *et al.* 2010; Ishishita *et al.*
765 2015; Mipam *et al.* 2023). However, the patterns we find in dwarf hamsters suggests that
766 spermatogenesis may be disrupted between zygotene and diplotene cell stages from early
767 misexpression. Dwarf hamster hybrid diplotene cell populations had X-linked and autosomal
768 gene expression profiles which more closely resemble parental leptotene/zygotene cell
769 populations than either diplotene or postmeiotic cell populations. Furthermore, transgressive

770 DE genes in hybrids during diplotene were enriched for genes associated with cell
771 differentiation, proliferation, and programmed cell death, suggesting misexpression during this
772 stage could be a consequence of a stalling or breakdown of early meiosis in hybrid dwarf
773 hamsters. It's unclear what underlying genomic mechanisms could result in this breakdown,
774 but it is possible that this disruption could potentially act as a major contributor to hybrid
775 sterility in this system. Ultimately, we find that spermatogenesis is a complex and rapidly
776 evolving developmental program that may provide many potential avenues across its timeline
777 for the evolution of hybrid incompatibilities.
778

779 **Abnormal sex chromosome expression patterns differ between dwarf hamster and house**
780 **mouse hybrids**

781 The sex chromosomes play a central role in speciation, an observation which has been
782 supported by both Haldane's rule (Haldane 1922) and the large X-effect on hybrid male sterility
783 (Coyne and Orr 1989). Misregulation of the X chromosome may contribute to hybrid sterility in
784 several species pairs (Davis *et al.* 2015; Morgan *et al.* 2020; Sánchez-Ramírez *et al.* 2021). The
785 X chromosome is transcriptionally repressed during routine spermatogenesis in many
786 organisms including eutherian mammals (McKee and Handel 1993), monotremes (Murat *et al.*
787 2023), *Drosophila* (Landeen *et al.* 2016), grasshoppers (Viera *et al.* 2021), mosquitos (Taxiarchi
788 *et al.* 2019), and nematodes (Rappaport *et al.* 2021). Because of the ubiquity of X chromosome
789 repression during spermatogenesis, disruption of transcriptional repression could be a
790 widespread regulatory phenotype in sterile hybrids (Lifschytz and Lindsley 1972; Larson *et al.*
791 2018). In sterile hybrid mice, disrupted X repression (disrupted MSCI) leads to the
792 overexpression of the normally silenced X chromosome during diplotene (Good *et al.* 2010;
793 Bhattacharyya *et al.* 2013; Campbell *et al.* 2013; Turner and Harr 2014; Larson *et al.* 2017,
794 2022). We also found overexpression of the X chromosome during diplotene in sterile hybrid

795 dwarf hamsters, but in a manner inconsistent with sterile hybrid house mice. Both the X
796 chromosome and autosomes are overexpressed in dwarf hamster hybrid diplotene cell
797 populations to a greater extent on average than was observed in house mice, and importantly,
798 X-linked overexpression was more variable in dwarf hamster hybrids than house mice hybrids.
799 In fact, some dwarf hamster hybrids had wildly overexpressed X chromosomes while others
800 appeared to have properly silenced X chromosomes. Our expression correlation and gene set
801 analyses of hybrid diplotene cell populations provide additional evidence that the genes
802 overexpressed in hybrid hamster diplotene are different than those overexpressed in house
803 mouse hybrids, sharing more similarity to the earlier meiotic cell types than downstream
804 postmeiotic cell types. Overall, our results indicate fundamentally different patterns of X-linked
805 overexpression in both systems, with X-linked overexpression in dwarf hamster hybrids being
806 inconsistent with disrupted MSCI patterns observed in house mouse hybrids.

807 Much of what we know about the genomic architecture and the role of sex
808 chromosome misregulation in hybrid male sterility in mammals comes from decades of work
809 that have shown a major gene, *Prdm9*, and its X chromosome modulator, *Hstx2*, may be
810 responsible for most F1 hybrid male sterility in house mice (Forejt *et al.* 1991, 2021; Trachtulec
811 *et al.* 1997; Mihola *et al.* 2009; Lustyk *et al.* 2019). *Prdm9* directs the location of double strand
812 breaks during meiotic recombination (Mihola *et al.* 2009; Oliver *et al.* 2009; Smagulova *et al.*
813 2016). In hybrid mice, divergence at *Prdm9* binding sites leads to asymmetric double-stranded
814 breaks and results in autosomal asynapsis, triggering Meiotic Silencing of Unsynapsed
815 Chromatin, shutting down transcription on asynapsed autosomes using the same cellular
816 machinery as MSCI (Turner 2015), and eventually meiotic arrest and cell death (Bhattacharyya
817 *et al.* 2013; Forejt *et al.* 2021). This process is associated with the disruption of MSCI and a
818 characteristic overexpression of the X chromosome during meiosis (Good *et al.* 2010;
819 Bhattacharyya *et al.* 2013; Campbell *et al.* 2013; Turner and Harr 2014; Larson *et al.* 2017,

820 2022), but whether disrupted MSCI directly contributes to hybrid male sterility or is simply a
821 downstream consequence of *Prdm9* divergence is still uncertain (Forejt *et al.* 2021).
822 Whether we should have expected patterns of disrupted sex chromosome expression
823 in sterile hybrid hamsters to be the same as house mice is unclear. The sex chromosomes in
824 pachytene cells of hybrid dwarf hamsters display normal yH2AFX staining (Ishishita *et al.* 2015;
825 Bikchurina *et al.* 2018), a key marker in MSCI (Abe *et al.* 2022), which may indicate that the
826 hybrid sex chromosomes are properly silenced. Additionally, autosomal asynapsis is rarely
827 observed in hybrid dwarf hamsters, and asynapsis is almost exclusive to the sex chromosomes
828 (Ishishita *et al.* 2015; Bikchurina *et al.* 2018). This contrasts *Prdm9*-mediated sterility in house
829 mice, where hybrid autosomes are often asynapsed and decorated with yH2AFX
830 (Bhattacharyya *et al.* 2013; Forejt *et al.* 2021). Mechanisms other than *Prdm9* may also disrupt
831 MSCI and result in sterility, such as macrosatellite copy number divergence (Bredemeyer *et al.*
832 2021) and X-autosome translocations that impair synapsis (Homolka *et al.* 2007), although
833 there is no evidence for X-autosome translocations between these two species of dwarf
834 hamsters (Moore *et al.* 2022). Thus, while MSCI may be a major target for the accumulation of
835 reproductive barriers between species in many mammalian systems, either through *Prdm9*
836 divergence or alternative mechanisms, our results suggest that sterility in dwarf hamsters has a
837 more composite regulatory basis.
838 Another mechanism often proposed to underlie mammalian male hybrid sterility,
839 especially in rodents, is divergence in the PAR between parental species. The PAR is the only
840 portion of the sex chromosomes which can synapse during spermatogenesis, and it is still
841 unclear if the regulation of the PAR is uniformly detached from MSCI across divergent
842 mammalian sex chromosome systems (Raudsepp and Chowdhary 2015). We find no evidence
843 that PAR-specific misregulation is associated with hybrid sterility in dwarf hamsters. PAR
844 genes are not silenced in hybrids or parents, a pattern that is inconsistent with MSCI that has

extended to the PAR due to XY asynapsis, and further, expression of PAR genes in hybrids differs little from parental PAR expression. While we find no evidence that PAR misregulation *per se* is associated with hybrid sterility in this system, we cannot rule out the possibility that structural and sequence divergence between the PARs of *P. sungorus* and *P. campbelli* may be associated with hybrid sterility. Structural and sequence divergence in the PAR has been hypothesized to activate the meiotic spindle checkpoint by interfering with proper pairing of sex chromosomes (Burgoyne *et al.* 2009; Dumont 2017). The PAR evolves rapidly in rodents (White *et al.* 2012b; Raudsepp and Chowdhary 2015; Morgan *et al.* 2019), and this elevated divergence may underlie sex chromosome asynapsis and apoptosis in several hybrid mouse crosses (Matsuda *et al.* 1991; Oka *et al.* 2010; White *et al.* 2012a; Dumont 2017). Furthermore, divergence in the mouse PAR has been implicated in spermatogenic defects in crosses where *Prdm9*-divergence is minimal, such as between closely related subspecies (Dumont 2017) or in mice with genetically-modified *Prdm9* alleles (Davies *et al.* 2021). Meiosis is likely tolerant to some degree of divergence in the PAR (Morgan *et al.* 2019), but exact limits are currently unknown. At this time, thorough analysis of structural and sequence divergence between the PARs in dwarf hamsters is challenging as the PAR is notoriously difficult to assemble (but see Kasahara *et al.* 2022), and there are annotation gaps in the current assembly of the PAR in dwarf hamsters. In sum, we find no clear pattern of regulatory disruption of PAR genes in sterile hybrid dwarf hamsters, though this result may change pending further refinement of the PAR annotation.

Conclusions

Cell-specific approaches for quantifying expression phenotypes are powerful tools for providing insight into the underlying mechanisms behind hybrid dysfunction (Hunnicutt *et al.* 2022), especially in systems where it remains difficult to interrogate the underlying genomic

870 architecture of these traits. Using a contrast of dwarf hamster and house mouse hybrids, we
871 have shown that transgressive overexpression is not an inevitable outcome of hybridization,
872 that misexpression resulting from hybrid incompatibilities may be likely to arise in differing
873 stages of spermatogenesis, and that disrupted sex chromosome silencing does not appear to
874 play an equal role in sterility between these two systems. Both the expression phenotypes we
875 observed here and histological evidence from other studies (Ishishita *et al.* 2015; Bikchurina *et*
876 *al.* 2018) suggest that several reproductive barriers are acting during spermatogenesis in dwarf
877 hamster hybrids. It has become increasingly apparent as more study systems are investigated
878 that the genetic basis of postzygotic species barriers are often complex and polymorphic
879 (Cutter 2012; Coughlan and Matute 2020), and implementing approaches which account for
880 the developmental complexities of hybrid dysfunction, as we have done here, will allow us to
881 make further advances in understanding the processes of speciation.
882

883 **Acknowledgements:**

884 This work was supported by a National Science Foundation Graduate Research Fellowship to
885 KEH (DGE-2034612) and the following grants awarded to KEH: Sigma Xi Grant-in-aid of
886 Research, American Society of Mammalogists Grant-in-Aid of Research Grant, and a Society
887 for the Study of Evolution R.C. Lewontin Early Award. Additionally, this work was supported by
888 grants from the Eunice Kennedy Shriver National Institute of Child Health and Human
889 Development of the National Institutes of Health (R01-HD073439, R01-HD094787) to JMG, and
890 the National Science Foundation to ELL (DEB-2012041). We would like to thank members of
891 the Larson and Good labs, as well as Jonathan Velotta and members of the Velotta lab, for
892 feedback on this project, Gabrielle Welsh for technical assistance, Ivan Kovanda for support
893 using the University of Denver Research Data Analysis Cluster, and Pamela K. Shaw and the
894 UM Fluorescence Cytometry Core supported by an Institutional Development Award from the

NIGMS (P30GM103338). Any opinions, findings, and conclusions or recommendations expressed in this material are those of the author(s) and do not necessarily reflect the views of the National Science Foundation or the National Institutes of Health.

Author contributions:

KEH, JMG, and ELL conceived of the study. CC, SK, ELL, and KEH conducted lab work. KEH conducted the analyses. KEH and ELL wrote the manuscript with input from ECM, CC, SK, and JMG.

Data accessibility:

Hamster sequence data are available through the NCBI SRA under accession number PRJNA1024468, and mouse sequence data are available under SRA accession PRJNA296926. File S1 contains all supplemental figures. Code used for the analyses and fertility phenotypic data are available from GitHub (https://github.com/KelsieHunnicutt/dwarf_hamster_hybrids).

907 **LITERATURE CITED**
908

909 Abe H., Y.-H. Yeh, Y. Munakata, K.-I. Ishiguro, P. R. Andreassen, *et al.*, 2022 Active DNA
910 damage response signaling initiates and maintains meiotic sex chromosome
911 inactivation. Nat. Commun. 13: 7212.

912 Anders S., and W. Huber, 2010 Differential expression analysis for sequence count data.
913 Nature Precedings 1–1.

914 Barreto F. S., R. J. Pereira, and R. S. Burton, 2015 Hybrid dysfunction and physiological
915 compensation in gene expression. Mol. Biol. Evol. 32: 613–622.

916 Bayes J. J., and H. S. Malik, 2009 Altered heterochromatin binding by a hybrid sterility protein
917 in Drosophila sibling species. Science 326: 1538–1541.

918 Benjamini Y., and Y. Hochberg, 1995 Controlling the false discovery rate: a practical and
919 powerful approach to multiple testing. J. R. Stat. Soc. 57: 289–300.

920 Bhattacharyya T., S. Gregorova, O. Mihola, M. Anger, J. Sebestova, *et al.*, 2013 Mechanistic
921 basis of infertility of mouse intersubspecific hybrids. Proc. Natl. Acad. Sci. U. S. A. 110:
922 E468–E477.

923 Bikchurina T. I., K. V. Tishakova, E. A. Kizilova, S. A. Romanenko, N. A. Serdyukova, *et al.*,
924 2018 Chromosome synapsis and recombination in male-sterile and female-fertile
925 interspecies hybrids of the dwarf hamsters (Phodopus, Cricetidae). Genes 9: 227.

926 Bolger A. M., M. Lohse, and B. Usadel, 2014 Trimmomatic: a flexible trimmer for Illumina
927 sequence data. Bioinformatics 30: 2114–2120.

928 Bredemeyer K. R., C. M. Seabury, M. J. Stickney, J. R. McCarrey, B. M. vonHoldt, *et al.*, 2021

929 Rapid macrosatellite evolution promotes X-linked hybrid male sterility in a feline
930 interspecies cross. Mol. Biol. Evol. 38: 5588–5609.

931 Brekke T. D., and J. M. Good, 2014 Parent-of-origin growth effects and the evolution of hybrid
932 inviability in dwarf hamsters. Evolution 68: 3134–3148.

933 Brekke T. D., L. A. Henry, and J. M. Good, 2016 Genomic imprinting, disrupted placental
934 expression, and speciation. Evolution 70: 2690–2703.

935 Brekke T. D., K. A. Steele, and J. F. Mulley, 2018 Inbred or outbred? Genetic diversity in
936 laboratory rodent colonies. G3 8: 679–686.

937 Brekke T. D., E. C. Moore, S. C. Campbell-Staton, C. M. Callahan, Z. A. Cheviron, *et al.*, 2021 X
938 chromosome-dependent disruption of placental regulatory networks in hybrid dwarf
939 hamsters. Genetics 218: iyab043.

940 Burgoyne P. S., 1982 Genetic homology and crossing over in the X and Y chromosomes of
941 mammals. Hum. Genet. 61: 85–90.

942 Burgoyne P. S., S. K. Mahadevaiah, and J. M. A. Turner, 2009 The consequences of asynapsis
943 for mammalian meiosis. Nat. Rev. Genet. 10: 207–216.

944 Campbell P., J. M. Good, and M. W. Nachman, 2013 Meiotic sex chromosome inactivation is
945 disrupted in sterile hybrid male house mice. Genetics 193: 819–828.

946 Civetta A., 2016 Misregulation of gene expression and sterility in interspecies hybrids: causal
947 links and alternative hypotheses. J. Mol. Evol. 82: 176–182.

948 Coughlan J. M., and D. R. Matute, 2020 The importance of intrinsic postzygotic barriers
949 throughout the speciation process. Philos. Trans. R. Soc. Lond. B Biol. Sci. 375:

20190533.

Coyne J. A., and H. A. Orr, 1989 Two rules of speciation, pp. 180–207 in *Speciation and its consequences*, edited by Otte D., Endler J. A. Sinauer Associates, Sunderland, MA.

Cutter A. D., 2012 The polymorphic prelude to Bateson-Dobzhansky-Muller incompatibilities. Trends Ecol. Evol. 27: 209–218.

Cutter A. D., and J. D. Bundus, 2020 Speciation and the developmental alarm clock. Elife 9: e56276.

Danecek P., A. Auton, G. Abecasis, C. A. Albers, E. Banks, *et al.*, 2011 The variant call format and VCFtools. Bioinformatics 27: 2156–2158.

Davies B., E. Hatton, N. Altemose, J. G. Hussin, F. Pratto, *et al.*, 2016 Re-engineering the zinc fingers of PRDM9 reverses hybrid sterility in mice. Nature 530: 171–176.

Davies B., A. Gupta Hinch, A. Cebrian-Serrano, S. Alghadban, P. W. Becker, *et al.*, 2021 Altering the binding properties of PRDM9 partially restores fertility across the species boundary. Mol. Biol. Evol. 38: 5555–5562.

Davis B. W., C. M. Seabury, W. A. Brashear, G. Li, M. Roelke-Parker, *et al.*, 2015 Mechanisms underlying mammalian hybrid sterility in two feline interspecies models. Mol. Biol. Evol. 32: 2534–2546.

Dumont B. L., 2017 Meiotic consequences of genetic divergence across the murine pseudoautosomal region. Genetics 205: 1089–1100.

Ellis N., and P. N. Goodfellow, 1989 The mammalian pseudoautosomal region. Trends Genet. 5: 406–410.

971 Forejt J., V. Vincek, J. Klein, H. Lehrach, and M. Loudová-Micková, 1991 Genetic mapping of
972 the t-complex region on mouse chromosome 17 including the Hybrid sterility-1 gene.
973 Mamm. Genome 1: 84–91.

974 Forejt J., P. Jansa, and E. Parvanov, 2021 Hybrid sterility genes in mice (Mus musculus): a
975 peculiar case of PRDM9 incompatibility. Trends Genet. 37: 1095–1108.

976 Gamperl R., G. Vistorin, and W. Rosenkranz, 1977 New observations on the karyotype of the
977 Djungarian hamster, Phodopus sungorus. Experientia 33: 1020–1021.

978 Getun I. V., B. Torres, and P. R. J. Bois, 2011 Flow cytometry purification of mouse meiotic
979 cells. J. Vis. Exp. e2602.

980 Good J. M., M. A. Handel, and M. W. Nachman, 2008 Asymmetry and polymorphism of hybrid
981 male sterility during the early stages of speciation in house mice. Evolution 62: 50–65.

982 Good J. M., T. Giger, M. D. Dean, and M. W. Nachman, 2010 Widespread over-expression of
983 the X chromosome in sterile F1 hybrid mice. PLoS Genet. 6: e1001148.

984 Green C. D., Q. Ma, G. L. Manske, A. N. Shami, X. Zheng, *et al.*, 2018 A comprehensive
985 roadmap of murine spermatogenesis defined by single-cell RNA-Seq. Dev. Cell 46:
986 651-667.e10.

987 Gu Z., R. Eils, and M. Schlesner, 2016 Complex heatmaps reveal patterns and correlations in
988 multidimensional genomic data. Bioinformatics 32: 2847–2849.

989 Guerrero R. F., A. L. Posto, L. C. Moyle, and M. W. Hahn, 2016 Genome-wide patterns of
990 regulatory divergence revealed by introgression lines. Evolution 70: 696–706.

991 Haaf T., H. Weis, and M. Schmid, 1987 A comparative cytogenetic study on the mitotic and

992 meiotic chromosomes in hamster species of the genus Phodopus (Rodentia,
993 Cricetinae). Zeitschrift für Säugetierkunde 52: 281–290.

994 Haerty W., and R. S. Singh, 2006 Gene regulation divergence is a major contributor to the
995 evolution of Dobzhansky-Muller incompatibilities between species of Drosophila. Mol.
996 Biol. Evol. 23: 1707–1714.

997 Haldane J. B. S., 1922 Sex ratio and unisexual sterility in hybrid animals. J. Genet. 12: 101–
998 109.

999 Handel M. A., 2004 The XY body: a specialized meiotic chromatin domain. Exp. Cell Res. 296:
1000 57–63.

1001 Hermann B. P., K. Cheng, A. Singh, L. Roa-De La Cruz, K. N. Mutoji, *et al.*, 2018 The
1002 mammalian spermatogenesis single-cell transcriptome, from spermatogonial stem cells
1003 to spermatids. Cell Rep. 25: 1650-1667.e8.

1004 Holt J., S. Huang, L. McMillan, and W. Wang, 2013 Read annotation pipeline for high-
1005 throughput sequencing data, pp. 605–612 in *Proceedings of the International*
1006 *Conference on Bioinformatics, Computational Biology and Biomedical Informatics -*
1007 *BCB'13*, ACM Press, New York, New York, USA.

1008 Homolka D., R. Ivanek, J. Capkova, P. Jansa, and J. Forejt, 2007 Chromosomal rearrangement
1009 interferes with meiotic X chromosome inactivation. Genome Res. 17: 1431–1437.

1010 Huang S., J. Holt, C.-Y. Kao, L. McMillan, and W. Wang, 2014 A novel multi-alignment pipeline
1011 for high-throughput sequencing data. Database 2014: bau057.

1012 Hunnicutt K. E., J. M. Good, and E. L. Larson, 2022 Unraveling patterns of disrupted gene

1013 expression across a complex tissue. Evolution 76: 275–291.

1014 Ishishita S., K. Tsuboi, N. Ohishi, K. Tsuchiya, and Y. Matsuda, 2015 Abnormal pairing of X and
1015 Y sex chromosomes during meiosis I in interspecific hybrids of Phodopus campbelli
1016 and P. sungorus. Sci. Rep. 5: 9435.

1017 Kasahara T., K. Mekada, K. Abe, A. Ashworth, and T. Kato, 2022 Complete sequencing of the
1018 mouse pseudoautosomal region, the most rapidly evolving 'chromosome.' bioRxiv
1019 2022.03.26.485930.

1020 Kerwin R. E., and A. L. Sweigart, 2020 Rampant Misexpression in a Mimulus (Monkeyflower)
1021 Introgression Line Caused by Hybrid Sterility, Not Regulatory Divergence. Mol. Biol.
1022 Evol. 37: 2084–2098.

1023 Kim D., J. M. Paggi, C. Park, C. Bennett, and S. L. Salzberg, 2019 Graph-based genome
1024 alignment and genotyping with HISAT2 and HISAT-genotype. Nat. Biotechnol. 37: 907–
1025 915.

1026 Kolberg L., U. Raudvere, I. Kuzmin, J. Vilo, and H. Peterson, 2020 gprofiler2 -- an R package
1027 for gene list functional enrichment analysis and namespace conversion toolset
1028 g:Profiler. F1000Res. 9. https://doi.org/10.12688/f1000research.24956.2

1029 Kopania E. E. K., E. L. Larson, C. Callahan, S. Keeble, and J. M. Good, 2022a Molecular
1030 evolution across mouse spermatogenesis. Mol. Biol. Evol. 39: msac023.

1031 Kopania E. E. K., E. M. Watson, C. C. Rathje, B. M. Skinner, P. J. I. Ellis, *et al.*, 2022b The
1032 contribution of sex chromosome conflict to disrupted spermatogenesis in hybrid house
1033 mice. Genetics 222: iyac151.

1034 Korunes K. L., and K. Samuk, 2021 pixy: Unbiased estimation of nucleotide diversity and
1035 divergence in the presence of missing data. Mol. Ecol. Resour. 21: 1359–1368.

1036 Kousathanas A., D. L. Halligan, and P. D. Keightley, 2014 Faster-X adaptive protein evolution in
1037 house mice. Genetics 196: 1131–1143.

1038 Lafon-Placette C., and C. Köhler, 2015 Epigenetic mechanisms of postzygotic reproductive
1039 isolation in plants. Curr. Opin. Plant Biol. 23: 39–44.

1040 Landeen E. L., C. A. Muirhead, L. Wright, C. D. Meiklejohn, and D. C. Presgraves, 2016 Sex
1041 chromosome-wide transcriptional suppression and compensatory cis-regulatory
1042 evolution mediate gene expression in the Drosophila male germline. PLoS Biol. 14:
1043 e1002499.

1044 Larson E. L., D. Vanderpool, S. Keeble, M. Zhou, B. A. J. Sarver, *et al.*, 2016 Contrasting levels
1045 of molecular evolution on the mouse X chromosome. Genetics 203: 1841–1857.

1046 Larson E. L., S. Keeble, D. Vanderpool, M. D. Dean, and J. M. Good, 2017 The composite
1047 regulatory basis of the large X-effect in mouse speciation. Mol. Biol. Evol. 34: 282–295.

1048 Larson E. L., E. E. K. Kopania, and J. M. Good, 2018 Spermatogenesis and the evolution of
1049 mammalian sex chromosomes. Trends Genet. 34: 722–732.

1050 Larson E. L., E. E. K. Kopania, K. E. Hunnicutt, D. Vanderpool, S. Keeble, *et al.*, 2022 Stage-
1051 specific disruption of X chromosome expression during spermatogenesis in sterile
1052 house mouse hybrids. G3 12: jkab407.

1053 Liao Y., G. K. Smyth, and W. Shi, 2014 featureCounts: an efficient general purpose program for
1054 assigning sequence reads to genomic features. Bioinformatics 30: 923–930.

1055 Lifschytz E., and D. L. Lindsley, 1972 The role of X-chromosome inactivation during
1056 spermatogenesis. Proc. Natl. Acad. Sci. U. S. A. 69: 182–186.

1057 Llopart A., 2012 The rapid evolution of X-linked male-biased gene expression and the large-X
1058 effect in Drosophila yakuba, D. santomea, and their hybrids. Mol. Biol. Evol. 29: 3873–
1059 3886.

1060 Luo H., T. Mipam, S. Wu, C. Xu, C. Yi, *et al.*, 2022 DNA methylome of primary spermatocyte
1061 reveals epigenetic dysregulation associated with male sterility of cattleyak.
1062 Theriogenology 191: 153–167.

1063 Lustyk D., S. Kinský, K. K. Ullrich, M. Yancoskie, L. Kašíková, *et al.*, 2019 Genomic structure of
1064 Hstx2 modifier of Prdm9-dependent hybrid male sterility in mice. Genetics 213: 1047–
1065 1063.

1066 Mack K. L., P. Campbell, and M. W. Nachman, 2016 Gene regulation and speciation in house
1067 mice. Genome Res. 26: 451–461.

1068 Mack K. L., and M. W. Nachman, 2017 Gene regulation and speciation. Trends Genet. 33: 68–
1069 80.

1070 Matsuda Y., T. Hirobe, and V. M. Chapman, 1991 Genetic basis of X-Y chromosome
1071 dissociation and male sterility in interspecific hybrids. Proc. Natl. Acad. Sci. U. S. A. 88:
1072 4850–4854.

1073 McCarthy D. J., Y. Chen, and G. K. Smyth, 2012 Differential expression analysis of multifactor
1074 RNA-Seq experiments with respect to biological variation. Nucleic Acids Res. 40: 4288–
1075 4297.

1076 McKee B. D., and M. A. Handel, 1993 Sex chromosomes, recombination, and chromatin
1077 conformation. Chromosoma 102: 71–80.

1078 McManus C. J., J. D. Coolon, M. O. Duff, J. Eipper-Mains, B. R. Graveley, *et al.*, 2010
1079 Regulatory divergence in Drosophila revealed by mRNA-seq. Genome Res. 20: 816–
1080 825.

1081 Meiklejohn C. D., J. D. Coolon, D. L. Hartl, and P. J. Wittkopp, 2014 The roles of cis- and trans-
1082 regulation in the evolution of regulatory incompatibilities and sexually dimorphic gene
1083 expression. Genome Res. 24: 84–95.

1084 Michalak P., and M. A. F. Noor, 2003 Genome-wide patterns of expression in Drosophila pure
1085 species and hybrid males. Mol. Biol. Evol. 20: 1070–1076.

1086 Mihola O., Z. Trachtulec, C. Vlcek, J. C. Schimenti, and J. Forejt, 2009 A mouse speciation
1087 gene encodes a meiotic histone H3 methyltransferase. Science 323: 373–375.

1088 Mipam T., X. Chen, W. Zhao, P. Zhang, Z. Chai, *et al.*, 2023 Single-cell transcriptome analysis
1089 and in vitro differentiation of testicular cells reveal novel insights into male sterility of the
1090 interspecific hybrid cattle-yak. BMC Genomics 24: 149.

1091 Montgomery S. H., and J. E. Mank, 2016 Inferring regulatory change from gene expression: the
1092 confounding effects of tissue scaling. Mol. Ecol. 25: 5114–5128.

1093 Moore E. C., G. W. C. Thomas, S. Mortimer, E. E. K. Kopania, K. E. Hunnicutt, *et al.*, 2022 The
1094 evolution of widespread recombination suppression on the dwarf hamster (Phodopus) X
1095 chromosome. Genome Biol. Evol. 14: evac080.

1096 Morgan A. P., T. A. Bell, J. J. Crowley, and F. Pardo-Manuel de Villena, 2019 Instability of the

pseudoautosomal boundary in house mice. Genetics 212: 469–487.

Morgan K., B. Harr, M. A. White, B. A. Payseur, and L. M. Turner, 2020 Disrupted gene networks in subfertile hybrid house mice. Mol. Biol. Evol. 37: 1547–1562.

Mugal C. F., M. Wang, N. Backström, D. Wheatcroft, M. Ålund, *et al.*, 2020 Tissue-specific patterns of regulatory changes underlying gene expression differences among *Ficedula* flycatchers and their naturally occurring F1 hybrids. Genome Res. 30: 1727–1739.

Murat F., N. Mbengue, S. B. Winge, T. Trefzer, E. Leushkin, *et al.*, 2023 The molecular evolution of spermatogenesis across mammals. Nature 613: 308–316.

Namekawa S. H., P. J. Park, L.-F. Zhang, J. E. Shima, J. R. McCarrey, *et al.*, 2006 Postmeiotic sex chromatin in the male germline of mice. Curr. Biol. 16: 660–667.

Neumann K., J. Michaux, V. Lebedev, N. Yigit, E. Colak, *et al.*, 2006 Molecular phylogeny of the Cricetinae subfamily based on the mitochondrial cytochrome b and 12S rRNA genes and the nuclear vWF gene. Mol. Phylogenet. Evol. 39: 135–148.

Ogle D., and M. D. Ogle, 2017 Package ‘FSA.’ CRAN Repos 1–206.

Oka A., A. Mita, Y. Takada, H. Koseki, and T. Shiroishi, 2010 Reproductive isolation in hybrid mice due to spermatogenesis defects at three meiotic stages. Genetics 186: 339–351.

Oka A., and T. Shiroishi, 2014 Regulatory divergence of X-linked genes and hybrid male sterility in mice. Genes Genet. Syst. 89: 99–108.

Oka A., T. Takada, H. Fujisawa, and T. Shiroishi, 2014 Evolutionarily diverged regulation of X-chromosomal genes as a primal event in mouse reproductive isolation. PLoS Genet. 10: e1004301.

1118 Oksanen J., F. G. Blanchet, R. Kindt, P. Legendre, P. R. Minchin, *et al.*, 2013 Package 'vegan.'
1119 Community ecology package, version 2: 1–295.

1120 Oliver P. L., L. Goodstadt, J. J. Bayes, Z. Birtle, K. C. Roach, *et al.*, 2009 Accelerated evolution
1121 of the Prdm9 speciation gene across diverse metazoan taxa. PLoS Genet. 5: e1000753.

1122 Ortíz-Barrientos D., B. A. Counterman, and M. A. F. Noor, 2007 Gene expression divergence
1123 and the origin of hybrid dysfunctions. Genetica 129: 71–81.

1124 Paun O., M. F. Fay, D. E. Soltis, and M. W. Chase, 2007 Genetic and epigenetic alterations
1125 after hybridization and genome doubling. Taxon 56: 649–656.

1126 Presgraves D. C., 2008 Sex chromosomes and speciation in Drosophila. Trends Genet. 24:
1127 336–343.

1128 Ramm S. A., and L. Schärer, 2014 The evolutionary ecology of testicular function: size isn't
1129 everything. Biol. Rev. Camb. Philos. Soc. 89: 874–888.

1130 Rappaport Y., H. Achache, R. Falk, O. Murik, O. Ram, *et al.*, 2021 Bisection of the X
1131 chromosome disrupts the initiation of chromosome silencing during meiosis in
1132 Caenorhabditis elegans. Nat. Commun. 12: 4802.

1133 Raudsepp T., and B. P. Chowdhary, 2015 The eutherian pseudoautosomal region. Cytogenet.
1134 Genome Res. 147: 81–94.

1135 Raymond C. S., M. W. Murphy, M. G. O'Sullivan, V. J. Bardwell, and D. Zarkower, 2000 Dmrt1,
1136 a gene related to worm and fly sexual regulators, is required for mammalian testis
1137 differentiation. Genes Dev. 14: 2587–2595.

1138 Ritchie M. E., B. Phipson, D. Wu, Y. Hu, C. W. Law, *et al.*, 2015 limma powers differential

1139 expression analyses for RNA-sequencing and microarray studies. Nucleic Acids Res.
1140 43: e47.

1141 Robinson M. D., D. J. McCarthy, and G. K. Smyth, 2010 edgeR: a Bioconductor package for
1142 differential expression analysis of digital gene expression data. Bioinformatics 26: 139–
1143 140.

1144 Sánchez-Ramírez S., J. G. Weiss, C. G. Thomas, and A. D. Cutter, 2021 Widespread
1145 misregulation of inter-species hybrid transcriptomes due to sex-specific and sex-
1146 chromosome regulatory evolution. PLoS Genet. 17: e1009409.

1147 Scribner S. J., and K. E. Wynne-Edwards, 1994 Disruption of body temperature and behavior
1148 rhythms during reproduction in dwarf hamsters (Phodopus). Physiol. Behav. 55: 361–
1149 369.

1150 Shivaprasad P. V., R. M. Dunn, B. A. Santos, A. Bassett, and D. C. Baulcombe, 2012
1151 Extraordinary transgressive phenotypes of hybrid tomato are influenced by epigenetics
1152 and small silencing RNAs. EMBO J. 31: 257–266.

1153 Smagulova F., K. Brick, Y. Pu, R. D. Camerini-Otero, and G. V. Petukhova, 2016 The
1154 evolutionary turnover of recombination hot spots contributes to speciation in mice.
1155 Genes Dev. 30: 266–280.

1156 Swanson M. T., C. H. Oliveros, and J. A. Esselstyn, 2019 A phylogenomic rodent tree reveals
1157 the repeated evolution of masseter architectures. Proc. Biol. Sci. 286: 20190672.

1158 Taxiarchi C., N. Kranjc, A. Kriezis, K. Kyrou, F. Bernardini, *et al.*, 2019 High-resolution
1159 transcriptional profiling of Anopheles gambiae spermatogenesis reveals mechanisms of
1160 sex chromosome regulation. Sci. Rep. 9: 14841.

1161 Trachtulec Z., M. Mnuková-Fajdelová, R. M. Hamvas, S. Gregorová, W. E. Mayer, *et al.*, 1997
1162 Isolation of candidate hybrid sterility 1 genes by cDNA selection in a 1.1 megabase pair
1163 region on mouse chromosome 17. Mamm. Genome 8: 312–316.

1164 Turner L. M., M. A. White, D. Tautz, and B. A. Payseur, 2014 Genomic networks of hybrid
1165 sterility. PLoS Genet. 10: e1004162.

1166 Turner L. M., and B. Harr, 2014 Genome-wide mapping in a house mouse hybrid zone reveals
1167 hybrid sterility loci and Dobzhansky-Muller interactions. Elife 3: e02504.

1168 Turner J. M. A., 2015 Meiotic silencing in mammals. Annu. Rev. Genet. 49: 395–412.

1169 Vasimuddin M., S. Misra, H. Li, and S. Aluru, 2019 Efficient architecture-aware acceleration of
1170 BWA-MEM for multicore systems, pp. 314–324 in *2019 IEEE International Parallel and*
1171 *Distributed Processing Symposium (IPDPS)*, IEEE.

1172 Viera A., M. T. Parra, S. Arévalo, C. García de la Vega, J. L. Santos, *et al.*, 2021 X chromosome
1173 inactivation during grasshopper spermatogenesis. Genes 12: 1844.

1174 Wei K. H.-C., A. G. Clark, and D. A. Barbash, 2014 Limited gene misregulation is exacerbated
1175 by allele-specific upregulation in lethal hybrids between Drosophila melanogaster and
1176 Drosophila simulans. Mol. Biol. Evol. 31: 1767–1778.

1177 White M. A., M. Stubbings, B. L. Dumont, and B. A. Payseur, 2012a Genetics and evolution of
1178 hybrid male sterility in house mice. Genetics 191: 917–934.

1179 White M. A., A. Ikeda, and B. A. Payseur, 2012b A pronounced evolutionary shift of the
1180 pseudoautosomal region boundary in house mice. Mamm. Genome 23: 454–466.

1181 Wittkopp P. J., B. K. Haerum, and A. G. Clark, 2004 Evolutionary changes in cis and trans gene

1182 regulation. Nature 430: 85–88.

1183 Wu C. I., and A. W. Davis, 1993 Evolution of postmating reproductive isolation: the composite
1184 nature of Haldane's rule and its genetic bases. Am. Nat. 142: 187–212.

1185 Zhu W., B. Hu, C. Becker, E. S. Doğan, K. W. Berendzen, *et al.*, 2017 Altered chromatin
1186 compaction and histone methylation drive non-additive gene expression in an
1187 interspecific Arabidopsis hybrid. Genome Biol. 18: 157.